

21 NATURAL CLIMATE PROCESSES

Contents

- 21.1. Radiative Balance 793
 - 21.1.1. The So-called “Greenhouse Effect” 795
 - 21.1.2. Atmospheric Window 796
 - 21.1.3. Average Energy Budget 797
- 21.2. Astronomical Influences 797
 - 21.2.1. Milankovitch Theory 797
 - 21.2.2. Solar Output 803
- 21.3. Tectonic Influences 804
 - 21.3.1. Continent Movement 804
 - 21.3.2. Volcanism 804
- 21.4. Feedbacks 806
 - 21.4.1. Concept 806
 - 21.4.2. Idealized Example 807
 - 21.4.3. Infrared Radiative (IR) Feedback 810
 - 21.4.4. Water-vapor Feedback 810
 - 21.4.5. Lapse-rate Feedback 810
 - 21.4.6. Cloud Feedback 811
 - 21.4.7. Ice–albedo (Surface) Feedback 811
 - 21.4.8. Ocean CO₂ Feedback 812
 - 21.4.9. Biological CO₂ Feedback 812
- 21.5. Gaia Hypothesis & Daisyworld 813
 - 21.5.1. Physical Approximations 813
 - 21.5.2. Steady-state and Homeostasis 815
- 21.6. GCMs 815
- 21.7. Present Climate 816
 - 21.7.1. Definition 816
 - 21.7.2. Köppen Climate Classification 817
- 21.8. Natural Oscillations 818
 - 21.8.1. El Niño - Southern Oscillation (ENSO) 818
 - 21.8.2. Pacific Decadal Oscillation (PDO) 820
 - 21.8.3. North Atlantic Oscillation (NAO) 824
 - 21.8.4. Arctic Oscillation (AO) 824
 - 21.8.5. Madden-Julian Oscillation (MJO) 824
 - 21.8.6. Other Oscillations 824
- 21.9. Review 825
- 21.10. Homework Exercises 826
 - 21.10.1. Broaden Knowledge & Comprehension 826
 - 21.10.2. Apply 827
 - 21.10.3. Evaluate & Analyze 829
 - 21.10.4. Synthesize 832

The dominant climate process is radiation to and from the Earth-ocean-atmosphere system. Increased absorption of solar (shortwave) radiation causes the climate to warm, which is compensated by increased infrared (IR, longwave) radiation out to space. This strong negative feedback has allowed the absolute temperature at Earth’s surface to vary by only 4% over millions of years.

But small changes have indeed occurred. Recent changes are associated with human activity such as greenhouse-gas emissions and land-surface modification. Other changes are natural — influenced by astronomical and tectonic factors. These primary influences can be amplified or damped by changes in clouds, ice, vegetation, and other feedbacks.

To illustrate dominant processes, consider the following highly simplified “toy” models.

21.1. RADIATIVE BALANCE

Consider an Earth with no atmosphere (Fig. 21.1). Given the near-constant climate described above, assume a balance of radiation input and output.

Incoming solar radiation minus the portion reflected, multiplied by the area intercepted by Earth, gives the total radiative input:

$$\text{Radiation In} = (1 - A) \cdot S_0 \cdot \pi \cdot R_{\text{Earth}}^2 \quad \bullet(21.1)$$

where the fraction reflected ($A = 0.294$) is called the **global albedo** (see INFO Box). The annual-average **total solar irradiance (TSI)** over all wavelengths

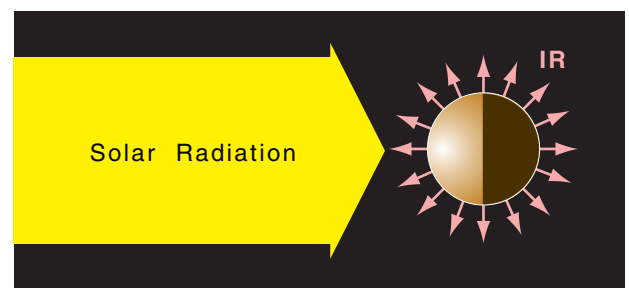


Figure 21.1

Earth’s radiation balance of solar energy in and infrared (IR) radiation out.



“Practical Meteorology: An Algebra-based Survey of Atmospheric Science” by Roland Stull is licensed under a Creative Commons Attribution-NonCommercial-ShareAlike 4.0 International License. View this license at <http://creativecommons.org/licenses/by-nc-sa/4.0/>. This work is available at https://www.eoas.ubc.ca/books/Practical_Meteorology/

INFO • Albedo

The average global reflectivity (portion of incoming sunlight that is reflected back to space) for Earth is called the **albedo**, A . But the exact value of A is difficult to measure, due to natural variability of cloud and snow cover, and due to calibration errors in the satellite radiation sensors.

Trenberth, Fasullo & Kiehl (2009, *Bul. Amer. Meteor. Soc.*) report a range of values of $27.9\% \leq A \leq 34.2\%$. The 2013 International Panel on Climate Change (IPCC) 5th Assessment Report (AR5) suggests $A \approx 29.4\%$, which we will use here.

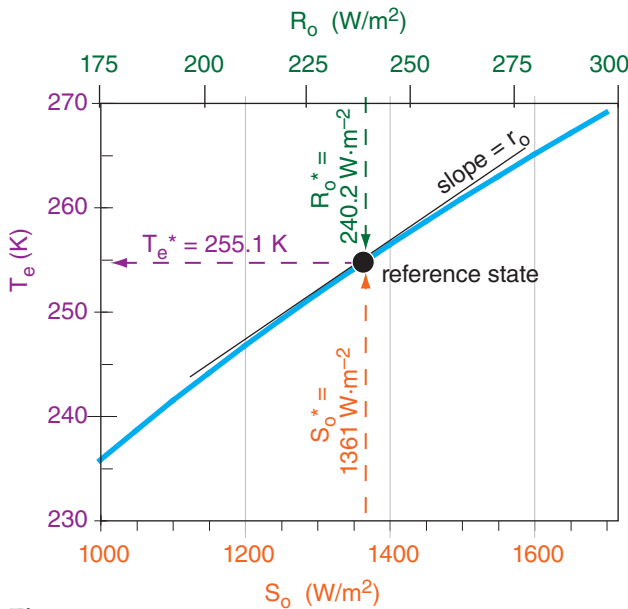


Figure 21.2 Thick curved cyan line shows how the effective radiation temperature T_e for Earth varies with changes in solar irradiance S_o , given global albedo $A = 0.294$. Dashed lines show present conditions, which will be used as a reference point or reference state (R_o^* , T_e^*). Thin black straight line shows the slope r_o of the curve at the reference point. $R_o = (1-A) \cdot S_o/4$ is net solar input for each square meter of the Earth’s surface (see INFO Box, next page).

Sample Application

Show the calculations leading to $T_e = -18.0^\circ\text{C}$.

Find the Answer:

Given: $T_e = -18.0^\circ\text{C}$, $S_o = 1361 \text{ W}\cdot\text{m}^{-2}$, $A = 0.294$

Find: Show the calculation

Use eq. (21.3):

$$T_e = \left[\frac{(1 - 0.294) \cdot (1361 \text{ W}\cdot\text{m}^{-2})}{4 \cdot (5.67 \times 10^{-8} \text{ W}\cdot\text{m}^{-2}\cdot\text{K}^{-4})} \right]^{1/4}$$

$$= 255.1 \text{ K} = \underline{-18.0^\circ\text{C}}$$

Check: Physics & units are OK.

Exposition: Earth’s radius appears in both the radiation-in and -out equations, but is not in eq. (21.3).

as measured by satellites is $S_o = 1361 \text{ W}\cdot\text{m}^{-2}$. The interception area is the same as the area of Earth’s shadow — a disk of area πR_{Earth}^2 , where $R_{Earth} = 6371 \text{ km}$ is the average radius of Earth. The TSI has fluctuated about $\pm 0.5 \text{ W}\cdot\text{m}^{-2}$ (the thickness of the vertical dashed line in Fig. 21.2) during the past 33 years due to the average sunspot cycle. See the Solar & IR Radiation chapter for TSI details.

IR radiation is emitted from every point on Earth’s surface, which we will assume to behave as a radiative blackbody (emissivity = 1). For this toy model, assume that the earth is spherical with surface area $4\pi R_{Earth}^2$. If IR emissions/area are given by the Stefan-Boltzmann law (eq. 2.15), then the total outgoing radiation is:

$$\text{Radiation Out} = 4\pi \cdot R_{Earth}^2 \cdot \sigma_{SB} \cdot T_e^4 \quad \bullet(21.2)$$

where the Stefan-Boltzmann constant is $\sigma_{SB} = 5.67 \times 10^{-8} \text{ W}\cdot\text{m}^{-2}\cdot\text{K}^{-4}$.

The real Earth has a heterogeneous surface with cold polar ice caps, warm tropical continents, and other temperatures associated with different terrestrial and aquatic geographic features. Define an **effective radiation emission temperature** (T_e) such that the emissions from a hypothetical earth of uniform surface temperature T_e is the same as the total heterogeneous-Earth emissions.

For a steady-state climate (i.e., no temperature change with time), outputs must balance the inputs. Thus, equate outgoing and incoming radiation from eqs. (21.1 and 21.2), and then solve the resulting equation for T_e :

$$T_e = \left[\frac{(1 - A) \cdot S_o}{4 \cdot \sigma_{SB}} \right]^{1/4} = \left[\frac{R_o}{\sigma_{SB}} \right]^{1/4} \quad \bullet(21.3)$$

$$\approx 255.1 \text{ K} \approx -18.0^\circ\text{C}$$

where $R_o = (1-A) \cdot S_o/4$.

Fig. 21.2 shows this **reference state** at 255.1K, given an albedo of 0.294. It also shows how changes of solar irradiance along the abscissa of the graph need only small changes in effective temperature along the ordinate in order to reach a new radiative equilibrium. Namely, the radiation balance describes a **negative feedback** that causes a stable climate rather than runaway global warming.

The geological record illustrates the steadiness of Earth’s past climate (Fig. 21.3). About 60 M years ago, the absolute temperature of Earth’s surface averaged roughly 5% warmer (i.e., $14 \text{ K} = 14^\circ\text{C}$ warmer) than present. For the most recent 10 k years, the geologic record indicates temperature oscillations on the order of $\pm 1^\circ\text{C}$ relative to our current average surface temperature of 15°C . Nonetheless,

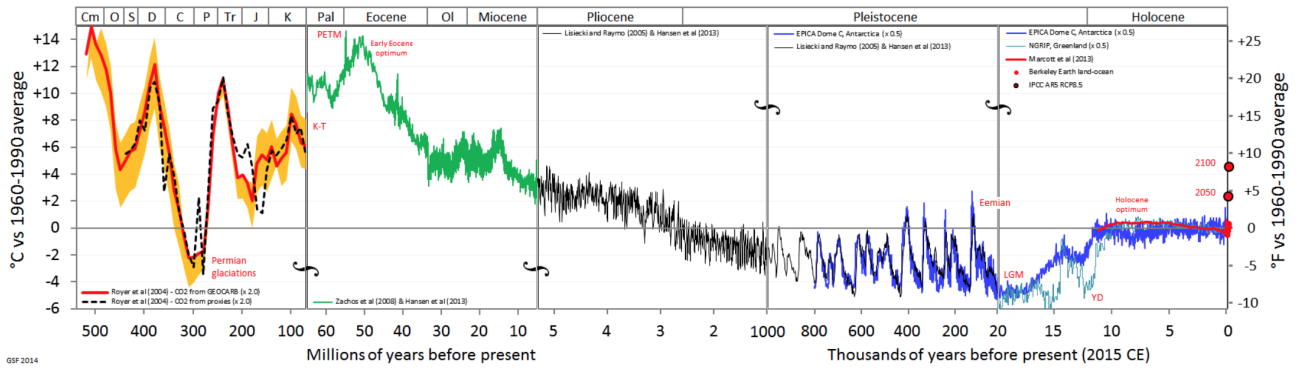


Figure 21.3

Paleotemperature estimate as a difference ΔT ($^{\circ}\text{C}$) from the 1960 to 1990 temperature average. Scale breaks at the vertical lines. Note the ice-age cycles during 20 - 1000 k years ago. (By Glen Fergus - Own work, CC BY-SA 3.0, <https://commons.wikimedia.org/w/index.php?curid=31736468>)

these small temperature changes (with ΔT range of 20°C over the past 500 Myr) can cause significant changes in ice-cap coverage and sea level.

But our simple toy model is perhaps too simple, because the modeled -18.0°C temperature is colder than the $+15^{\circ}\text{C}$ actual surface temperature (from Chapter 1). To improve the modeled temperature, we must include some additional physics.

21.1.1. The So-called “Greenhouse Effect”

To make our Earth-system model slightly more realistic, add an atmosphere of uniform absolute temperature T_A everywhere (Fig 21.4). Suppose this atmosphere is opaque (not transparent) in the IR, but is perfectly transparent for visible light.

For this idealized case, sunlight shines through the atmosphere and reaches the Earth’s surface, where a portion is reflected and a portion is absorbed, causing the surface to warm. IR emitted from the warm Earth is totally absorbed by the atmosphere, causing the atmosphere to warm. But the atmosphere also emits radiation: some upward to space, and some back down to the Earth’s surface (a surface that absorbs 100% of the IR that hits it).

This downward IR from the atmosphere adds to the solar input, thus allowing the Earth’s surface to have a greater surface temperature T_s than with no atmosphere. This is called the **greenhouse effect**, even though real greenhouses do not work this way. Water vapor is one of many “greenhouse gases” that absorbs and emits IR radiation.

Assume the atmosphere-Earth system has existed for sufficient years to reach a **steady state**. Such an equilibrium state requires outgoing IR from the atmosphere-Earth system to balance absorbed incoming solar radiation. Namely:

$$T_A = T_e = 255.1 \text{ K} = -18.0^{\circ}\text{C} \quad (21.4)$$

Thus, the temperature of the atmosphere must equal the **effective emission temperature** for the atmosphere-Earth system.

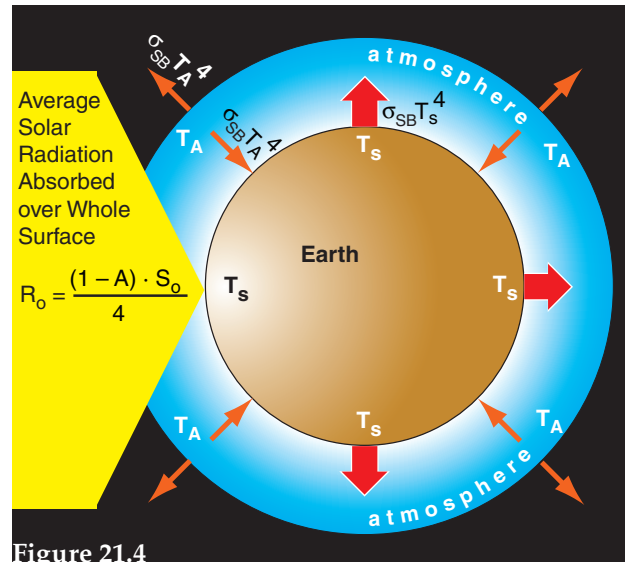


Figure 21.4

Simplified atmosphere-Earth system with greenhouse effect. Atmosphere thickness is exaggerated. R_0 is the net solar input.

INFO • Why does $R_0 = (1-A) \cdot S_0 / 4$?

In Figs. 21.4 and 21.5, the **net solar input** R_0 is given as $(1-A) \cdot S_0 / 4$ instead of S_0 . The $(1-A)$ factor is because any sunlight reflected back to space is not available to heat the Earth system. But why also divide by 4? The reason is due to geometry.

Of the radiation streaming outward from the sun, the shadow cast by the Earth indicates how much radiation was intercepted. The shadow is a circle with radius equal to the Earth’s radius R_{Earth} , hence the interception area is πR_{Earth}^2 .

But we prefer to study the energy fluxes relative to each square meter of the Earth’s surface. The surface area of a sphere is $4 \cdot \pi R_{Earth}^2$. Namely, the surface area is four times the area intercepted by the sun.

Hence, the average net solar input that we allocate to each square meter of the Earth’s surface is: $R_0 = (1-A) \cdot S_0 / 4 = (1-0.294) \cdot (1361 \text{ W} \cdot \text{m}^{-2}) / 4 = 240.2 \text{ W} \cdot \text{m}^{-2}$.

Sample Application

What temperature is the Earth’s surface for the one-layer atmosphere of the previous sample applic.

Find the Answer

Given: $T_e = 255.1 \text{ K}$
 Find: $T_s = ? \text{ K}$

Apply eq. (21.6): $T_s = 2^{1/4} \cdot (255.1 \text{ K}) = 303.4 \text{ K} = \underline{30.2^\circ\text{C}}$

Check: Physics and units are OK.

Exposition: Twice the radiation at Earth’s surface, but not twice the surface absolute temperature.

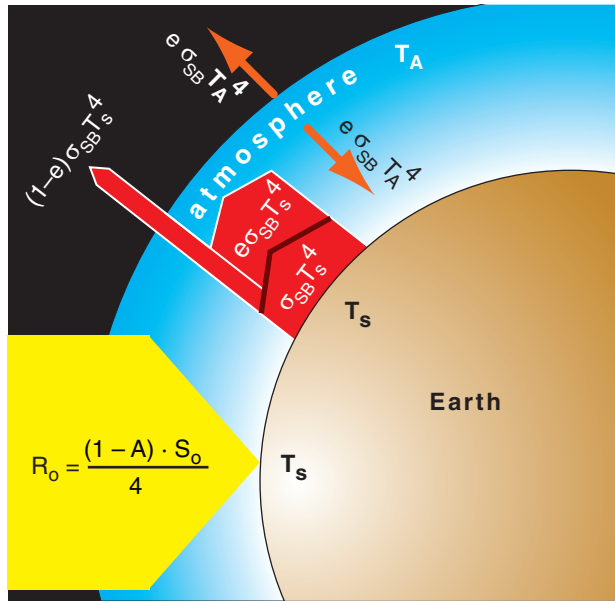


Figure 21.5
 Idealized single-layer atmosphere having an IR dirty window.

Sample Application

Given an idealized case similar to the previous Sample Application, but with a dirty atmospheric window having $e_\lambda = 0.899$. Find T_A and T_s .

Find the Answer

Given: $e_\lambda = 0.899$, and $T_e = 255.1 \text{ K}$,
 Find: $T_A = ? \text{ K}$, $T_s = ? \text{ K}$

Apply eq. (21.10):

$$T_s = \left(\frac{2}{2 - 0.899} \right)^{1/4} \cdot (255.1 \text{ K}) = 296.2 \text{ K} = \underline{23.0^\circ\text{C}}$$

From Eq. (21.7) we see that the effective emission temperature of the atmosphere is:

$$T_A = (0.5)^{1/4} \cdot T_s = 0.84 \cdot (296.2 \text{ K}) \approx 249.1 \text{ K} = \underline{-24.1^\circ\text{C}}$$

Check: Physics & units are OK.

Exposition: This simple “dirty window” model is better, but still does not give the desired T_s of 15°C .

You can use the Stefan-Boltzmann law $\sigma_{SB} \cdot T_A^4$ to find the radiation emitted both up and down from the atmosphere, which is assumed to be thin relative to Earth’s radius. For the atmosphere to be in steady-state, these two streams of outgoing IR radiation must balance the one stream of incoming IR from the Earth’s surface $\sigma_{SB} \cdot T_s^4$, which requires:

$$\sigma_{SB} \cdot T_s^4 = 2 \cdot \sigma_{SB} \cdot T_A^4 \quad (21.5)$$

Thus

$$T_s = 2^{1/4} \cdot T_e \quad \bullet(21.6)$$

$$= 303.4 \text{ K} = 30.2^\circ\text{C}$$

While the no-atmosphere case was too cold, this opaque-atmosphere case is too warm (recall from Chapter 1 that the standard atmosphere $T_s = 15^\circ\text{C}$). Perhaps the air is not fully opaque in the IR.

21.1.2. Atmospheric Window

As discussed in the Satellites & Radar chapter, Earth’s atmosphere is partially transparent (i.e., is a dirty **atmospheric window**) for the 8 to 14 μm range of infrared radiation (IR) wavelengths and is mostly opaque at other wavelengths. Of all the IR emissions upward from Earth’s surface, suppose that 89.9% is absorbed and 10.1% escapes to space (Fig. 21.5). Thus, the atmosphere will not warm as much, and in turn, will not re-emit as much radiation back to the Earth’s surface.

At each layer (Earth’s surface, atmosphere, space) outgoing and incoming radiative fluxes balance for an Earth-system in equilibrium. Also, fluxes out of one layer are input to an adjacent layer. For example, the radiative balance of the atmosphere becomes

$$e_\lambda \cdot \sigma_{SB} \cdot T_s^4 = 2 \cdot e_\lambda \cdot \sigma_{SB} \cdot T_A^4 \quad (21.7)$$

while at the Earth’s surface it is

$$R_0 + e_\lambda \cdot \sigma_{SB} \cdot T_A^4 = \sigma_{SB} \cdot T_s^4 \quad (21.8)$$

From Kirchhoff’s law (see the Solar & IR Radiation chapter), recall that absorptivity equals emissivity, which for this idealized case is $e_\lambda = a_\lambda = 89.9\%$. Eqs. (21.3, 21.7 & 21.8) can be combined to solve for key absolute temperatures:

$$T_A^4 = \frac{T_e^4}{2 - e_\lambda} \quad \bullet(21.9)$$

$$T_s^4 = \frac{2 \cdot T_e^4}{2 - e_\lambda} \quad \bullet(21.10)$$

where T_e is still given by eq. (21.4). The result is:

$$T_A \approx 249.1 \text{ K} = -24.1^\circ\text{C}$$

and

$$T_s \approx 296.2 \text{ K} = 23.0^\circ\text{C} \quad (21.11)$$

The temperature at Earth's surface is more realistic, but is still slightly too warm.

A by-product of human industry and agriculture is the emission of gases such as methane (CH₄), carbon dioxide (CO₂), freon CFC-12 (C Cl₂ F₂), and nitrous oxide (N₂O) into the atmosphere. These gases, known as **anthropogenic greenhouse gases**, can absorb and re-emit IR radiation that would otherwise have been lost out the dirty window. The resulting increase of IR emissions from the atmosphere to Earth's surface could cause **global warming**.

21.1.3. Average Energy Budget

Radiation is not the only physical process that transfers energy. Between the Earth and the bottom layer of the atmosphere there can be sensible-heat transfer via conduction (see the Thermodynamics chapter) and latent-heat transfer via evapotranspiration (see the Water Vapor chapter). Once this heat and moisture are in the air, they can be transported further into the atmosphere by the mean wind, by deep convection such as thunderstorms, by shallow convection such as thermals, and by smaller turbulent eddies in the atmospheric boundary layer.

One estimate of the annual mean of energy fluxes between all these components, when averaged over the surface area of the globe, is sketched in Fig. 21.6. According to the Stefan-Boltzmann law, the emitted IR radiation from the Earth's surface (398 W·m⁻²) corresponds to a blackbody surface temperature of 16.3°C, which is close to the observed value of 15°C.

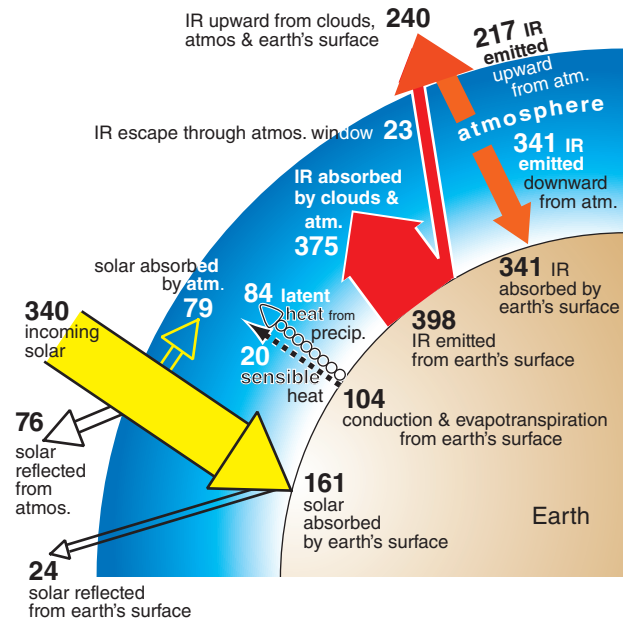


Figure 21.6

Approximate global annual mean energy budget for the Earth system. The “atmosphere” component includes the air, clouds, and particles in the air. Numbers are energy fluxes in units of W·m⁻² relative to the Earth’s surface. Errors are of order 3% for fluxes at the top of the atmosphere, and errors are 5 to 25% for surface fluxes. The incoming solar radiation, when averaged over all the Earth’s surface, is $S_0/4 = 340 \text{ W}\cdot\text{m}^{-2}$. After subtracting the outgoing (reflected) solar radiation ($340 - 76 - 24 = 240 \text{ W}\cdot\text{m}^{-2}$), the result is the same R_0 that we used before. [Based partially on IPCC AR5 Chapt. 2, Fig. 2.11, and Trenberth, Fasullo & Kiehl 2009, and Trenberth & Fasullo 2012. For sake of illustration, I modified the atmospheric IR emissions by 0.4% (within the reported noise range) to give a balanced budget. Instructors should encourage students to debate energy budget issues.]



21.2. ASTRONOMICAL INFLUENCES

If the incoming solar radiation (**insolation**) changes, then the radiation budget of the Earth will adjust, possibly altering the climate. Two causes of daily-averaged insolation \bar{E} change at the top of the atmosphere are changes in solar output S_0 and changes in Earth-sun distance R (recall eq. 2.21).

21.2.1. Milankovitch Theory

In the 1920s, astrophysicist Milutin Milankovitch proposed that slow fluctuations in the Earth’s orbit around the sun can change the sun-Earth distance. Distance changes alter insolation according to the inverse square law (eq. 2.16), thereby contributing to climate change. Ice-age recurrence (inferred from ice and sediment cores) was later found to be correlated with orbital characteristics, supporting his

Sample Application

Confirm that energy flows in Fig. 21.6 are balanced.

Find the Answer

Solar: incoming = [reflected] + (absorbed)
 $340 = [76 + 24] + (79 + 161)$
 $340 = 340 \text{ W}\cdot\text{m}^{-2}$

Earth’s surface: incoming = outgoing
 $(161 + 341) = (104 + 398)$
 $502 = 502 \text{ W}\cdot\text{m}^{-2}$

Atmosphere: incoming = outgoing
 $(79 + 20 + 84 + 375) = (217 + 341)$
 $558 = 558 \text{ W}\cdot\text{m}^{-2}$

Earth System: in from space = out to space
 $340 = (24 + 76 + 23 + 217)$
 $340 = 340 \text{ W}\cdot\text{m}^{-2}$

Check: Yes, all budgets are balanced.

Exposition: The solar budget must balance because the Earth-atmosphere system does not create/emit solar radiation. However, IR radiation is created by the sun, Earth, and atmosphere; hence, the IR fluxes by themselves need not balance.

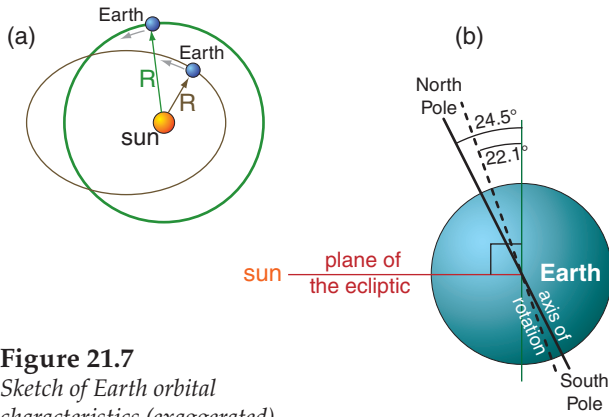


Figure 21.7
Sketch of Earth orbital characteristics (exaggerated).
(a) Eccentricity variations. Green line shows a circular orbit. Thin black line is an elliptical orbit. (b) Obliquity variations.

Sample Application
Plot ellipses for eccentricities of 0, 0.005, 0.058 & 0.50.
Hints: the (x, y) coordinates are given by $x = a \cos(t)$, and $y = b \sin(t)$, where t varies from 0 to 2π radians. Assume a semi-major axis of $a = 1$, and get the semi-minor axis from $b = a(1 - e^2)^{1/2}$.

Find the Answer
Plotted at right:

Exposition. The first 3 curves (solid green lines) look identical. Thus, for the full range of Earth's eccentricities ($0.0034 \leq e \leq 0.58$), we see that Earth's orbit is nearly circular ($e = 0$).

Sample Application.
Approximate the Earth-orbit eccentricity 600,000 years ago (i.e., 600,000 years before year 2000) using $N = 5$.

Find the Answer.
Given: $t = -600,000$ years (negative sign for past).
Find: e (dimensionless).

Use eq. (21.12) with data from Table 21-1:

$$e \approx 0.0275579 + 0.010739 \cdot \cos[2\pi(-600000\text{yr}/405091\text{yr} + 170.739^\circ/360^\circ)] + 0.008147 \cdot \cos[2\pi(-600000\text{yr}/94932\text{yr} + 109.891^\circ/360^\circ)] + 0.006222 \cdot \cos[2\pi(-600000\text{yr}/123945\text{yr} - 60.044^\circ/360^\circ)] + 0.005287 \cdot \cos[2\pi(-600000\text{yr}/98857\text{yr} - 86.140^\circ/360^\circ)] + 0.004492 \cdot \cos[2\pi(-600000\text{yr}/130781\text{yr} + 100.224^\circ/360^\circ)]$$

$$e \approx 0.0275579 + 0.0107290 + 0.0081106 + 0.0062148 - 0.0019045 - 0.0016384 \approx \mathbf{0.049}$$
 (dimensionless)

Check: $0.0034 \leq e \leq 0.058$, within the expected eccentricity range for Earth. Almost agrees with the exact answer of 0.047 from Fig. 21.8, using all $N = 20$ terms.

Exposition: An **interglacial** (non-ice-age) period was ending, & a new **glacial** (ice-age) period was starting.

hypothesis. Milankovitch focused on three orbital characteristics: eccentricity, obliquity, and precession.

21.2.1.1. Eccentricity

The shape of Earth's elliptical orbit around the sun (Fig. 21.7a) slowly fluctuates between nearly circular (**eccentricity** $e \approx 0.0034$) and slightly elliptical ($e \approx 0.058$). For comparison, a perfect circle has $e = 0$. Gravitational pulls by other planets (mostly Jupiter and Saturn) cause these eccentricity fluctuations.

Earth's eccentricity at any time (past or future) can be calculated using a sum of N cosine terms:

$$e \approx e_0 + \sum_{i=1}^N A_i \cdot \cos \left[C \cdot \left(\frac{t}{P_i} + \frac{\phi_i}{360^\circ} \right) \right] \quad \bullet(21.12)$$

where $e_0 = 0.0275579$ and t is time in years relative to calendar year 2000. For each cosine term (i.e., for each i index from 1 to N), use the orbital factors given in Table 21-1b (at the end of this chapter, in section 21.10.3), where A_i are amplitudes, P_i are oscillation periods in years, ϕ_i are phase shifts in degrees. C should be either 360° or 2π radians, depending on the trigonometric argument required by your calculator, spreadsheet, or programming language.

Fig. 21.8 shows eccentricity (purple curve at top) calculated using all 20 terms, for times ranging from 1 million years in the past to 1 million years into the future.

index	A	P (years)	ϕ (degrees)
Eccentricity:			
i= 1	0.010739	405,091.	170.739
2	0.008147	94,932.	109.891
3	0.006222	123,945.	-60.044
4	0.005287	98,857.	-86.140
5	0.004492	130,781.	100.224
Obliquity:			
j= 1	0.582412°	40,978.	86.645
2	0.242559°	39,616.	120.859
3	0.163685°	53,722.	-35.947
4	0.164787°	40,285.	104.689
Climatic Precession:			
k= 1	0.018986	23,682.	44.374
2	0.016354	22,374.	-144.166
3	0.013055	18,953.	154.212
4	0.008849	19,105.	-42.250
5	0.004248	23,123.	90.742

Simplified from Laskar, Robutel, Joutel, Gastineau, Correia & Levrard, 2004: A long-term numerical solution for the insolation quantities of the Earth. "Astronomy & Astrophysics", 428, 261-285.

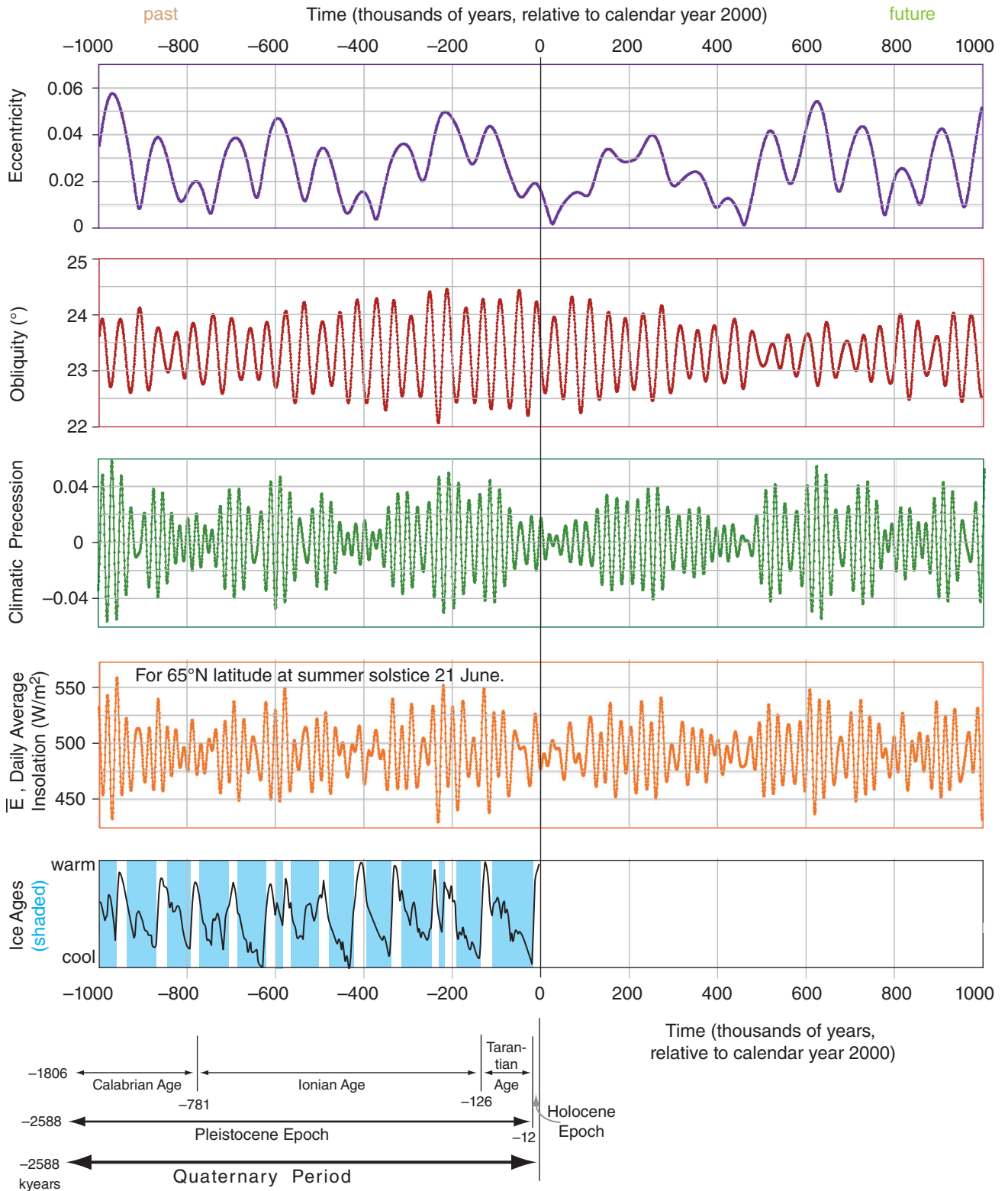


Figure 21.8

Past and future orbital characteristics in Milankovitch theory, as calculated using all the terms (see Table 21-1b at end of this chapter) in the series approximations of eqs. (21.12 - 21.20). Bottom curve shows relative temperature changes estimated from ice and sediment cores. Ice ages (glacial periods) are shaded cyan. Precession is for the summer solstice (i.e., only the $e \cdot \sin(\omega)$ term is used). Data points every 500 years in the top 4 graphs were found using calculations from the web page provided by Laskar and colleagues, updated on 15 August 2015 by M. Gastineau. <http://vo.imcce.fr/insola/earth/online/earth/online/index.php>

Sample Application

Estimate Earth’s obliquity 90,000 yrs in the future (relative to calendar year 2000) using $N = 4$.

Find the Answer

Given: $t = 90,000$ yr (positive sign indicates future)
 Find: $\epsilon = ?^\circ$

Use eq. (21.13) with coefficients from Table 21-1.

$$\begin{aligned} \epsilon &= 23.2545^\circ \\ &+ 0.582412^\circ \cdot [2\pi(90000\text{yr}/40978\text{yr} + 86.645^\circ/360^\circ)] \\ &+ 0.242559^\circ \cdot [2\pi(90000\text{yr}/39616\text{yr} + 120.859^\circ/360^\circ)] \\ &+ 0.163685^\circ \cdot [2\pi(90000\text{yr}/53722\text{yr} - 35.947^\circ/360^\circ)] \\ &+ 0.164787^\circ \cdot [2\pi(90000\text{yr}/40285\text{yr} + 104.689^\circ/360^\circ)] \end{aligned}$$

$$\begin{aligned} \epsilon &= 23.2545^\circ - 0.537349^\circ - 0.189273^\circ - 0.145639^\circ - 0.162777^\circ \\ &= \underline{\underline{22.219^\circ}} \end{aligned}$$

Check: Units OK. Within Earth range $22.1^\circ \leq \epsilon \leq 24.5^\circ$.

Exposition: Almost agrees with the exact answer of 22.268° from Fig. 21.8. At this small obliquity, seasonal contrasts are smaller than at present, allowing glaciers to grow due to cooler summers.

By eye, we see two superimposed oscillations of eccentricity with periods of about 100 and 400 kyr (where “kyr” = kilo years = 1000 years). The first oscillation correlates very well with the roughly 100 kyr period for cool events associated with **ice ages**. The present eccentricity is about 0.0167. Short-term forecast: eccentricity will change little during the next 100,000 years. Variations in e affect Earth-sun distance R via eq. (2.4) in the Solar & IR Radiation chapter.

21.2.1.2. Obliquity

The tilt (obliquity) of Earth’s axis slowly fluctuates between 22.1° and 24.5° . This tilt angle is measured from a line perpendicular to Earth’s orbital plane (the ecliptic) around the sun (Fig. 21.7b).

A series approximation for obliquity ϵ is:

$$\epsilon = \epsilon_0 + \sum_{j=1}^N A_j \cdot \cos \left[C \cdot \left(\frac{t}{P_j} + \frac{\phi_j}{360^\circ} \right) \right] \quad \bullet(21.13)$$

where $\epsilon_0 = 23.254500^\circ$, and all the other factors have the same meaning as for the eq. (21.12). Table 21-1 shows values for these orbital factors for $N = 4$ terms in this series, and Table 21-1b has all $N = 23$ terms.

The red curve in Fig. 21.8 shows that obliquity oscillates with a period of about 41,000 years. The present obliquity is 23.439° and is gradually decreasing.

Obliquity affects insolation via the solar declination angle (eq. 2.5 in the Solar & IR Radiation chapter, where a different symbol Φ_f was used for obliquity). Recall from the Solar & IR Radiation chapter that Earth-axis tilt is responsible for the seasons, so greater obliquity would cause greater contrast between winter and summer. One hypothesis is that ice ages are more likely during times of lesser obliquity, because summers would be cooler, causing less melting of glaciers.

21.2.1.3. Precession

Various precession processes affect climate.

Axial Precession. Not only does the tilt magnitude (obliquity) of Earth’s axis change with time, but so does the tilt direction. This tilt direction rotates in space, tracing one complete circle in 25,680 years (Fig. 21.9a) relative to the fixed stars. It rotates opposite to the direction the Earth spins. This precession is caused by the gravitational pull of the sun and moon on the Earth, because the Earth is an oblate spheroid (has larger diameter at the equator than at the poles). Hence, the Earth behaves somewhat like a spinning toy top.

Aphelion Precession. The direction of the major axis of Earth’s elliptical orbit also precesses slowly (with a 174,000 to 304,00 year period) relative to

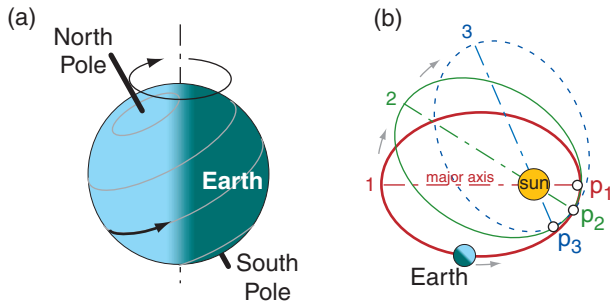


Figure 21.9

Sketch of additional Earth orbital characteristics. (a) Precession of Earth’s axis. (b) Precession of the orbit-ellipse major axis (aphelion precession) at successive times 1 - 3. Small white dots p_1, p_2, p_3 show locations of the perihelion (point on Earth’s orbit closest to sun). All the orbit ellipses are in the same plane.

the fixed stars (Fig. 21.9b). The rotation direction is the same as the axial-precession, but the precession speed fluctuates due to the gravitational pull of the planets (mostly Jupiter and Saturn).

Equinox Precession. Summing axial and aphelion precession rates (i.e., adding the inverses of their periods) gives a total precession with fluctuating period of about 22,000 years. This combined precession describes changes to the angle (measured at the sun) between Earth’s orbital positions at the perihelion (point of closest approach) and at the moving vernal (Spring) equinox (Fig. 21.10). This fluctuating angle (ϖ , a math symbol called “variant pi”) is the equinox precession.

For years when angle ϖ is such that the winter solstice is near the perihelion (as it is in this century), then the cooling effect of the N. Hemisphere being tilted away from the sun is slightly moderated by the fact that the Earth is closest to the sun; hence winters and summers are not as extreme as they could be. Conversely, for years with different angle ϖ such that the summer solstice is near the perihelion, then the N. Hemisphere is tilted toward the sun at the same time that the Earth is closest to the sun — hence expect hotter summers and colder winters. However, seasons near the perihelion are shorter duration than seasons near the aphelion, which moderates the extremes for this latter case.

Climatic Precession. ϖ by itself is less important for insolation than the combination with eccentricity e : $e \cdot \sin(\varpi)$ and $e \cdot \cos(\varpi)$. These terms, known as the climatic precession, can be expressed by series approximations, where both terms use the same coefficients from Table 21-1b, for $N = 26$.

$$e \cdot \sin(\varpi) \approx \sum_{k=1}^N A_k \cdot \sin \left[C \cdot \left(\frac{t}{P_k} + \frac{\Phi_k}{360^\circ} \right) \right] \quad \bullet(21.14)$$

$$e \cdot \cos(\varpi) \approx \sum_{k=1}^N A_k \cdot \cos \left[C \cdot \left(\frac{t}{P_k} + \frac{\Phi_k}{360^\circ} \right) \right] \quad (21.15)$$

Other factors are similar to those in eq. (21.12).

A plot of eq. (21.14), labeled “climatic precession”, is shown as the green curve in Fig. 21.8. It shows high frequency (22,000 year period) waves with amplitude modulated by the eccentricity curve from the top of Fig. 21.8. Climatic precession affects sun-Earth distance, as described next.

21.2.1.4. Insolation Variations

Eq. (2.21) from the Solar & IR Radiation chapter gives average daily insolation \bar{E} . It is repeated here: •(21.16)

$$\bar{E} = \frac{S_0}{\pi} \cdot \left(\frac{a}{R} \right)^2 \cdot \left[h_0' \cdot \sin(\phi) \cdot \sin(\delta_s) + \cos(\phi) \cdot \cos(\delta_s) \cdot \sin(h_0) \right]$$

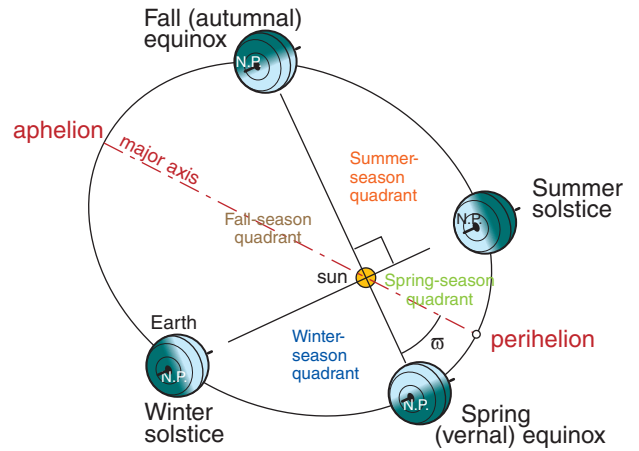


Figure 21.10
Illustration for sometime in the future, showing the angle (ϖ) of the perihelion from the moving vernal equinox. N.P. = North Pole. Seasons are for the N. Hemisphere. Tilt of the Earth’s axis is exaggerated to illustrate seasonal effects.

Sample Application

Estimate the sine term of the climatic precession for year 2000, for $N = 5$.

Find the Answer

Given: $t = 0$

Find: $e \cdot \sin(\varpi) = ?$ (dimensionless)

Use eq. (21.14) with coefficients from Table 21-1.

$$e \cdot \sin(\varpi) = + 0.018986 \cdot [2\pi \cdot (0\text{yr}/23682\text{yr} + 44.374^\circ/360^\circ)] + 0.016354 \cdot [2\pi \cdot (0\text{yr}/22374\text{yr} - 144.166^\circ/360^\circ)] + 0.013055 \cdot [2\pi \cdot (0\text{yr}/18953\text{yr} + 154.212^\circ/360^\circ)] + 0.008849 \cdot [2\pi \cdot (0\text{yr}/19105\text{yr} - 42.250^\circ/360^\circ)] + 0.004248 \cdot [2\pi \cdot (0\text{yr}/23123\text{yr} + 90.742^\circ/360^\circ)]$$

$$e \cdot \sin(\varpi) = 0.0132777 - 0.0095743 + 0.0056795 - 0.0059498 + 0.0042476 = \mathbf{0.00768}$$

Check: This value is smaller than the exact value of 0.01628 from the curve plotted in Fig. 21.8.

Exposition: The eccentricity in year 2000 (i.e., almost at present) causes medium climatic precession.

Table 21-2. Key values of λ , the angle between the Earth and the moving vernal equinox. Fig. 21.10 shows that solstices and equinoxes are exactly 90° apart.

Date	λ (radians, °)	$\sin(\lambda)$	$\cos(\lambda)$
Vernal (Spring) equinox	0, 0	0	1
Summer solstice	$\pi/2$, 90°	1	0
Autumnal (Fall) equinox	π , 180°	0	-1
Winter solstice	$3\pi/2$, 270°	-1	0

Sample Application

For the summer solstice at 65°N latitude, find the average daily insolation for years 2000 and 2200, using the small number of N values given in Table 21-1.

Find the Answer

Given: $\lambda = \pi/2$, $\phi = 65^\circ\text{N}$, (a) $t = 0$, (b) $t = 200$ yr
 Find: $\bar{E} = ? \text{ W m}^{-2}$ (Assume $S_o = 1361 \text{ W m}^{-2} = \text{const.}$)

(a) From previous statements and Sample Applications: $e = 0.0167$, $\delta_s = \varepsilon = 23.439^\circ$, $e \cdot \sin(\varpi) = 0.00768$

Use eq. (21.17): $h_o = \arccos[-\tan(65^\circ) \cdot \tan(23.439^\circ)]$
 $= 158.4^\circ = 2.7645 \text{ radians} = h_o'$

Eq. (21.20): $(a/R) = (1+0.00768)/[1-(0.0167)^2] = 1.00796$

Plugging all these into eq. (21.16):

$$\bar{E} = [(1361 \text{ W m}^{-2})/\pi] \cdot (1.00796)^2 \cdot [2.7645 \cdot \sin(65^\circ) \cdot \sin(23.439^\circ) + \cos(65^\circ) \cdot \cos(23.439^\circ) \cdot \sin(158.4^\circ)]$$

$$\bar{E} = 501.48 \text{ W m}^{-2} \text{ for } t = 0.$$

(b) Eq. (21.12) for $t = 200$: $e \approx 0.0168$

Eq. (21.13): $\varepsilon = 23.2278^\circ$. Eq. (21.14): $e \cdot \sin(\varpi) = 0.00730$

Eq. (21.20): $a/R = 1.00758$. Eq. (21.16): $\bar{E} = 497.5 \text{ W m}^{-2}$

Check: Units OK. Magnitude \approx that in Fig. 2.11 (Ch. 2) at the summer solstice (relative Julian day = 172).

Exposition: Milankovitch theory indicates that insolation will decrease slightly during the next 200 yr.

where $S_o = 1361 \text{ W m}^{-2}$ is the solar irradiance, $a = 149.457 \text{ Gm}$ is the semi-major axis length, R is the sun-Earth distance for any day of the year, h_o' is the hour angle in radians, ϕ is latitude, and δ_s is solar declination angle. Factors in this eq. are given next.

Instead of solving this formula for many latitudes, climatologists often focus on one key latitude: $\phi = 65^\circ\text{N}$. This latitude crosses Alaska, Canada, Greenland, Iceland, Scandinavia, and Siberia, and is representative of genesis zones for ice caps.

The hour angle h_o at sunrise and sunset is given by the following set of equations:

$$\alpha = -\tan(\phi) \cdot \tan(\delta_s) \tag{21.17a}$$

$$\beta = \min[1, (\max(-1, \alpha))] \tag{21.17b}$$

$$h_o = \arccos(\beta) \tag{21.17c}$$

Although the hour angle h_o can be in radians or degrees (as suits your calculator or spreadsheet), the hour angle marked with the prime (h_o' , in eq. 21.16) must be in radians.

The solar declination angle, used in eq. (21.16), is

$$\delta_s = \arcsin[\sin(\varepsilon) \cdot \sin(\lambda)] \approx \varepsilon \cdot \sin(\lambda) \tag{21.18}$$

where ε is the obliquity from eq. (21.13), and λ is the **true longitude** angle (measured at the sun) between the position of the Earth and the position of the moving **vernal equinox**. Special cases for λ are listed in Table 21-2 on the previous page.

Recall from the Solar & IR Radiation chapter (eq. 2.4) that the sun-Earth distance R is related to the semi-major axis a by:

$$\frac{a}{R} = \frac{1 + e \cdot \cos(v)}{1 - e^2} \tag{21.19}$$

where v is the true anomaly (the angle at the sun between the Earth's position and the perihelion), and e is the eccentricity. For the special case of the summer solstice (see the Sun-Earth Distance INFO Box), this becomes:

$$\frac{a}{R} = \frac{1 + [e \cdot \sin(\varpi)]}{1 - e^2} \tag{21.20}$$

where e is from eq. (21.12) and $e \cdot \sin(\varpi)$ is from eq. (21.14)

All the information above was used to solve eq. (21.16) for average daily insolation at latitude 65°N during the summer solstice for 1 Myr in the past to 1 Myr in the future. This results in the orange curve for \bar{E} plotted in Fig. 21.8. This is the climatic signal resulting from Milankovitch theory. Some scientists have found a good correlation between it and the

INFO • Sun-Earth Distance

Recall from Chapter 2 (eq. 2.4) that the sun-Earth distance R is related to the semi-major axis a by:

$$\frac{a}{R} = \frac{1 + e \cdot \cos(v)}{1 - e^2} \tag{21.19}$$

where v is the true anomaly (angle at the sun between Earth's position and the perihelion), and e is the eccentricity from eq. (21.12). By definition, $v = \lambda - \varpi$ (21.a) where λ is the position of the Earth relative to the moving vernal equinox, and ϖ is the position of the perihelion as measured from the moving vernal equinox. Thus,

$$\frac{a}{R} = \frac{1 + e \cdot \cos(\lambda - \varpi)}{1 - e^2} \tag{21.b}$$

Using trigonometric identities, the cosine term is:

$$\frac{a}{R} = \frac{1 + \cos(\lambda) \cdot [e \cdot \cos(\varpi)] + \sin(\lambda) \cdot [e \cdot \sin(\varpi)]}{1 - e^2} \tag{21.c}$$

The terms in square brackets are the **climatic precessions** that you can find with eqs. (21.14) and (21.15).

To simplify the study of climate change, researchers often consider a special time of year; e.g., the **summer solstice** ($\lambda = \pi/2$ from Table 21-2). This time of year is important because it is when glaciers may or may not melt, depending on how warm the summer is. At the summer solstice, the previous equation simplifies to:

$$\frac{a}{R} = \frac{1 + [e \cdot \sin(\varpi)]}{1 - e^2} \tag{21.20}$$

Also, during the summer solstice, the solar declination angle from eq. (21.18) simplifies to: $\delta_s = \varepsilon$

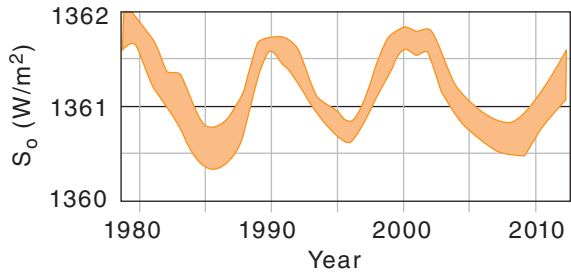


Figure 21.11
 Variation of annual average total solar irradiance S_o at the top of Earth's atmosphere during 3 recent sunspot cycles. [Based on data from IPCC (2013) AR5 Chapter 8, fig8.10, p689.]

historical temperature curve plotted at the bottom of Fig. 21.8, although the issue is still being debated.

21.2.2. Solar Output

The average total solar irradiance (TSI) currently reaching the top of Earth's atmosphere is $S_o = 1361 \text{ W}\cdot\text{m}^{-2}$, but the magnitude fluctuates daily due to solar activity, with extremes of 1358 and 1363 $\text{W}\cdot\text{m}^{-2}$ measured by satellite since 1975. Satellite observations have calibration errors (biases) on the order of $\pm 4.5 \text{ W}\cdot\text{m}^{-2}$ (Kopp & Lean, 2011, Fig. 1).

21.2.2.1. Sunspot Cycle

When averaged over each year, the resulting smoothed curve of TSI varies with a noticeable 11-yr cycle (Fig. 21.11), corresponding to the 9.5 to 11-yr sunspot cycle (Fig. 21.12) as observed by telescope.

Sunspots are darker and colder than the average surface temperature of the sun. However, sunspots are accompanied by faculae, which are brighter, hotter regions that often surround each sunspot. More sunspots means more faculae, and more faculae mean greater TSI.

Because the TSI variation is only about 0.1% of its total magnitude, the sunspot cycle is believed to have only a minor (possibly negligible) effect on recent climate change.

21.2.2.2. Long-term Variations in Solar Output

To get solar output information for the centuries before telescopes were invented, scientists use **proxy** measures. Proxies are measurable phenomena that vary with solar activity, such as beryllium-10 concentrations in Greenland ice cores, or carbon-14 concentration in tree rings (**dendrochronology**). Radioactive carbon-14 dating suggests solar activity as plotted in Fig. 21.13 for the past 1,000 years. Noticeable is the 200-yr cycle in solar-activity minima.

Going back 10,000 yr in time, Fig. 21.14 shows a highly-smoothed carbon-14 (^{14}C) estimate of solar/sunspot activity. There is some concern among sci-

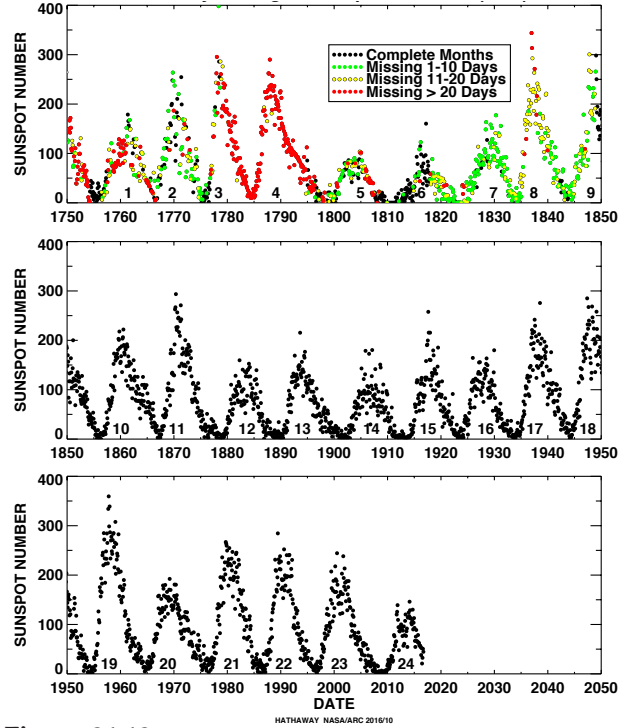


Figure 21.12
 Monthly average sunspot number during 1750 - 2017. [NASA. https://solarscience.msfc.nasa.gov/images/Zurich_Color.pdf]

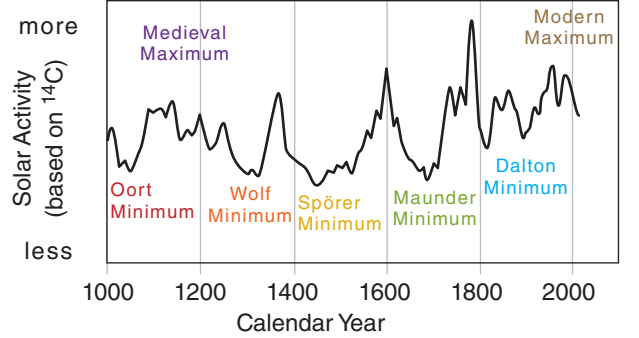


Figure 21.13
 Carbon-14 concentration as a proxy for solar activity. Approximate dates for these minima: **Oort Minimum:** 1040 - 1080, **Wolf Minimum:** 1280 - 1350, **Spörer Minimum:** 1450 - 1550, **Maunder Minimum:** 1645 - 1715, and **Dalton Minimum:** 1790 - 1830. The 11-year sunspot cycle still exists during this time span, but was smoothed out for this plot. (Based on data from Muscheler et al, 2007, *Quat.Sci.Rev.*, 26.)

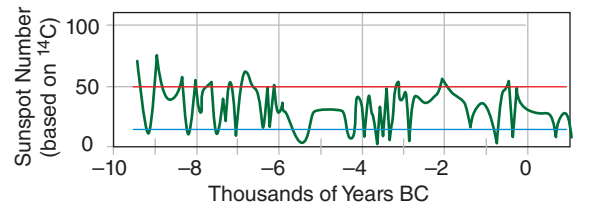


Figure 21.14
 Smoothed proxy estimate of sunspots, where the 11-year sunspot cycle has been averaged out. [Based on data from Usoskin, I.G. *Living Rev. Sol. Phys.* (2013) 10: 1. <https://doi.org/10.12942/lrsp-2013-1>]

entists that Earth-based factors (such as extensive volcanic eruptions that darken the sky and reduce tree growth over many decades) may have confounded the proxy analysis of tree rings.

Even further back (4.5 Gyr ago), the sun was younger and weaker, and emitted only about 70% of what it currently emits. About 5 billion years into the future, the sun will grow into a red-giant star (killing all life on Earth), and later will shrink to become a white dwarf star.



Figure 21.15
Location of continents about 225 million years ago when they were combined as the supercontinent Pangea (also spelled as Pangaea and Pangæa). This supercontinent spanned north-south from pole to pole.

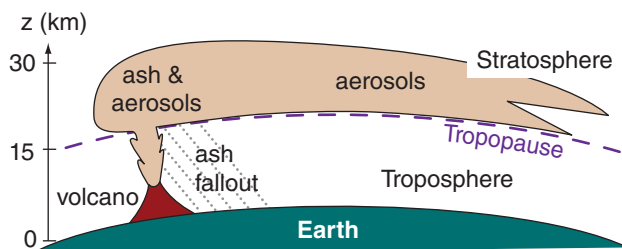


Figure 21.16
Eruption of volcanic ash and aerosols into the stratosphere. Average times for particles to fall 1 km are: 36 yr for 0.1 μm diameter particles, 3.2 yr for 0.5 μm , 328 days for 1 μm , 89 days for 2 μm , 14.5 days for 5 μm , and 3.6 days for 10 μm .

21.3. TECTONIC INFLUENCES

21.3.1. Continent Movement

As Earth-crust tectonic plates move, continents form, change, merge and break apart. About 225 million years ago the continents were merged into the **Pangea** supercontinent (Fig. 21.15). The interior of such large continents are sufficiently far from the moderating influence of oceans that extreme daily and seasonal temperature variations can occur. Large monsoon circulations can form due to the temperature contrasts between continent and ocean. The more recent (200 million years ago) supercontinents of Gondwanaland and Laurasia would likely have had similar monsoon circulations, and extreme temperature variations in their interiors.

Colliding tectonic plates can cause **mountain building (orogenesis)**. Large mountain ranges can block portions of the global circulation, changing the Rossby waves in the jet stream, and altering cyclogenesis regions. Mountains can partially block the movement of airmasses, changing temperature and precipitation patterns.

Changes in continent locations and ocean depths cause changes in ocean circulations. **Thermohaline** circulations are driven by differences in water-density caused by temperature and salt-concentration variations. These large, slow circulations connect deep water and surface waters of all oceans, and are important for redistributing the excess heat from the equator toward the poles (see Fig. 11.14 in Chapter 11). Climatic changes in ocean-surface temperatures can alter atmospheric temperature, humidity, winds, cloudiness, and precipitation distribution.

21.3.2. Volcanism

When volcanoes erupt explosively, the eruptive heat and vertical momentum ejects tons of tiny rock particles called **volcanic ash** into the upper troposphere and lower stratosphere (Fig. 21.16). During the few weeks before this ash falls out of the air, it can block some sunlight from reaching the surface.

Gases such as **sulfur dioxide (SO_2)** are also emitted in large volumes (0.1 to 50×10^6 metric tons from the larger eruptions; see Fig. 21.17a), and are much more important for climate change. SO_2 oxidizes in the atmosphere to form sulfuric acid and sulfate **aerosols**, tiny droplets that fall so slowly they seem suspended in the air.

Those sulfate particles in the stratosphere can remain suspended in the atmosphere for a few years as they are spread around the world by the winds. The sulfates absorb and reflect some of the incom-

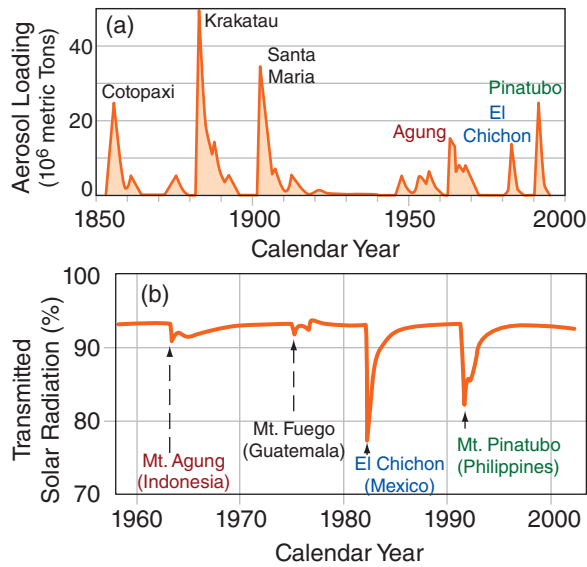


Figure 21.17
 Reduction in transmitted shortwave radiation from the sun due to aerosols and particulates erupted into the atmosphere from volcanoes, as observed at Mauna Loa. [Based on data from Sato et al., 1993. JGR, 98(D12), 22987–22994, doi:10.1029/93JD02553.]

ing solar radiation, allowing less to be transmitted toward the ground (Fig. 21.17b). Also, these aerosols absorb upwelling IR radiation from the Earth and troposphere.

The net result for aerosol particle diameters less than 0.5 μm is that the stratosphere warms while the Earth’s surface and lower troposphere cool. This cooling causes short-term (2 - 3 yr) climate change known as **volcanic winter** (analogous to the effects of **nuclear winter**). The surface cooling can be so great as to ruin vegetation and crops around the world, as was experienced throughout history (Table 21-3). For a brief explosive eruption, the stratospheric effects are greatest initially and gradually diminish over a 3-year period as the aerosols fall out. For violent continuous eruptions, the climatic effects can last decades to millennia.

Volcanoes also erupt hundreds of millions of tons of **greenhouse gases** (gases that absorb IR radiation that can alter the global heat budget), including carbon dioxide (CO₂) and water vapor (H₂O). These gases can cause longer-term global warming after the aerosol-induced cooling has ended.

After the large eruptions, you can see amazingly beautiful sunsets and sunrises with a bright **red glow** in the sky. Sometimes you can see a **blue moon** at night. These phenomena are due to scattering of sunlight by sulfate aerosols with diameters ≤ 0.5 μm (see the Atmospheric Optics chapter).

Table 21-3. Some notable volcanic eruptions.

Volcano (Date, Location) • Effect
Siberian Traps , creating floods of basaltic lava (~250 Myr ago, Russia) - Lasted a million years, emitting tremendous volumes of sulfates and greenhouse gases into the atmosphere that caused a mass extinction at the Permian-Triassic geological-period boundary. Known as the “ Great Dying ”, where 96% of all marine species and 70 percent of terrestrial vertebrate species disappeared. Major volcanic eruptions likely contributed to other mass extinctions: End-Ordovician (~450 Myr ago) and Late Devonian (~375 Myr ago).
Deccan Traps , creating floods of basaltic lava (~65.5 Myr ago, India) • The Cretaceous–Paleogene extinction event (K–Pg event, formerly known as Cretaceous–Tertiary or K-T event) was when the dinosaurs disappeared (except for those that evolved into modern-day birds). The sulfate and greenhouse-gas emissions from this massive eruption are believed to be a contributing factor to the K-T event, which was exacerbated by a massive asteroid impact in Mexico.
Yellowstone Caldera (640 kyr ago, USA) • Emissions reduced N. Hem. temperatures by about 5°C
Lake Toba (~90 kyr ago, Indonesia) • Emissions killed most of the humans on Earth, possibly causing a genetic bottleneck of reduced genetic diversity. Stratospheric aerosol load ≈ 1000 Mtons. Optical depth τ ≈ 10 (see Atmospheric Optics chapter for definition of τ).
Mt. Tambora (1815, Indonesia) • Emissions caused so much cooling in the N. Hemisphere that 1816 is known as the “ Year Without Summer ”. Widespread famine in Europe and N. America due to crop failure and livestock deaths. Followed by an exceptionally cold winter. Stratospheric aerosol load ≈ 200 Mtons. Optical depth τ ≈ 1.3.
Krakatau (1883, Indonesia) • Violent explosion heard 3,500 km away. Ash reached 80 km altitude. Global temperature decrease ≈ 0.3 - 1.2°C. 50 Mtons of aerosols into stratosphere. τ ≈ 0.55.

Darkness

“I had a dream, which was not all a dream.
 The bright sun was extinguish’d, and the stars
 Did wander darkling in the eternal space,
 Rayless, and pathless, and the icy Earth
 Swung blind and blackening in the moonless air;
 Morn came and went — and came, and
 brought no day,
 And men forgot their passions in the dread
 Of this their desolation; and all hearts
 Were chill’d into a selfish prayer for light.”

- Lord Byron (1816 –the Year Without Summer.)

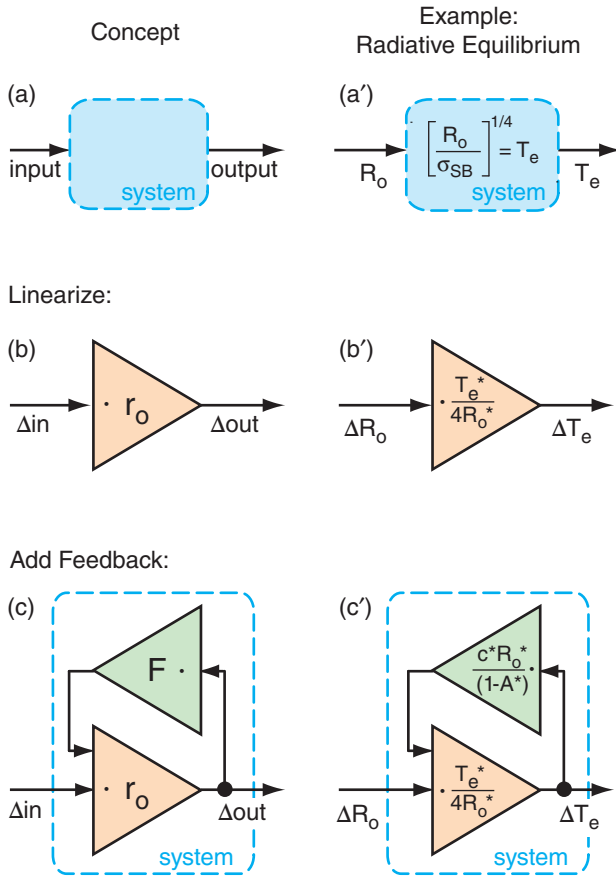


Figure 21.18
 Left column: feedback concepts. Right column: example of ice-albedo feedback within the radiative-equilibrium process, as described by nonlinear eq. (21.3). The reference state is (R_o^*, T_e^*, A^*, c^*) .

Sample Application
 Suppose $r_o = 0.1$ and $F = -3$. Find the feedback factor, gain, and compare system responses with and without feedback.

Find the Answer
 Given: $F = -3$, no-feedback system response $r_o = 0.1$
 Find: $f = ?$, $G = ?$, $r = ?$ = response with feedback

Use eq. (21.24):
 $f = (0.1) \cdot (-3) = \mathbf{-0.3}$ is the feedback factor

Use eq. (21.26):
 $G = 1 / [1 - (-0.3)] = \mathbf{0.77}$ is the gain

Use eq. (21.28):
 $r = (0.77) \cdot (0.1) = \mathbf{0.077}$ is the system response with feedback, compared to $r_o = 0.1$ without.

Check: Units all dimensionless. Magnitudes OK.

Exposition: This system is damped. It has negative feedback. This feedback diminishes the response. For many systems, the output units differ from the input units, in which case r_o , F , and r would have units.

21.4. FEEDBACKS

21.4.1. Concept

Consider a system or physical process with an input and output (Fig. 21.18a). This system might be **linear** (described by a straight line when output is plotted vs. input) or **nonlinear** (described by a curved line). Various values of input give various values of output.

Choose one particular set of input and output values as a **reference state** of the system. Find the slope r_o of the line at this reference point. This slope describes the **response** of the output (Δout) to a small change of input (Δin). Namely,

$$\Delta out = r_o \cdot \Delta in \tag{21.21}$$

as sketched in Fig. 21.18b. The slope is a straight line. Thus, even if the original system is nonlinear, this slope describes a **linearized approximation** to the system response at the reference point.

Feedback (Fig. 21.18c) is where the output signal is added to the input via some feedback process F :

$$\Delta out = r_o \cdot [\Delta in + F \cdot \Delta out] \tag{21.22}$$

A linear approximation is also used for this feedback. The feedback is internal to the system (Fig. 21.18c). Thus the amount of feedback responds to changes in the system. Contrast that to inputs, which are considered **external forcings** that do not respond to changes within the system.

The previous feedback equation can be rewritten as

$$\Delta out = r_o \cdot \Delta in + f \cdot \Delta out \tag{21.23}$$

where the **feedback factor** f is given by

$$f = r_o \cdot F \tag{21.24}$$

Solving eq. (21.33) for Δout gives:

$$\Delta out = \frac{1}{(1 - f)} \cdot r_o \cdot \Delta in \tag{21.25}$$

Eq. (21.25) looks similar to eq. (21.21) except for the new factor $1/(1-f)$. In electrical engineering, this factor is called the **gain**, G :

$$G = \frac{1}{(1 - f)} \tag{21.26}$$

[CAUTION: Some climate researchers use a different definition of gain than electrical engineers. See the INFO Box on the next page.]

If we rewrite eq. (21.25) as

$$\Delta_{out} = r \cdot \Delta_{in} \quad (21.27)$$

then we see that the linearized process WITH feedback (eq. 21.27) looks identical to that without (eq. 21.21) but with a different **response**:

$$r = G \cdot r_o \quad (21.28)$$

If $f \geq 1$, then the feedback is so strong that the response increases without limit (i.e., a **runaway** response), and no equilibrium exists. If $0 < f < 1$, then there is **positive feedback** with gain $G > 1$ that leads to an amplified but stable new equilibrium. If $f < 0$, then there is **negative feedback** with gain $G < 1$ that damps the response toward a different stable equilibrium.

For N feedback processes that are independent of each other and additive, the total gain is

$$G = \left[1 - \sum_{i=1}^N f_i \right]^{-1} \quad (21.29)$$

where f_i is the feedback factor for any one process i .

21.4.2. Idealized Example

To illustrate feedback, use the simple no-atmosphere blackbody radiative-equilibrium system of Fig. 21.1. The net solar input per square meter of the Earth’s surface is

$$R_o = (1 - A) \cdot S_o / 4 \quad (21.30)$$

(see the INFO box on the 3rd page of this chapter). The IR-radiation output is described by the Stefan-Boltzmann law, resulting in the following energy balance of input = output:

$$R_o = \sigma_{SB} \cdot T_e^4 \quad (21.31)$$

as indicated in Fig. 21.18a’.

The dashed lines in Fig. 21.2 show how an input of $R_o = 240.2 \text{ W m}^{-2}$ ($S_o = 1361 \text{ W m}^{-2}$) results in an output $T_e \approx 255.1 \text{ K}$. Use this blackbody Earth-equilibrium condition as the **reference state**, and denote the reference values with asterisks (R_o^*, T_e^*). The thick cyan curved line in Fig. 21.2 shows how T_e varies nonlinearly for different inputs of R_o , assuming $A = 0.294$ is constant (i.e., no feedback other than the background outgoing IR).

21.4.2.1. No Feedback

Focus on this no-feedback example first (Fig. 21.18b’). For small solar-input variations ΔR_o about its reference state, the corresponding temperature

INFO • Gain — Different Definitions

Some climate researchers define the **gain** g as

$$g = \frac{\Delta_{out} - \Delta_{out}_o}{\Delta_{out}}$$

where Δ_{out}_o is the background response with NO feedbacks. Thus:

$$g = \frac{G \cdot r_o \cdot \Delta_{in} - r_o \cdot \Delta_{in}}{G \cdot r_o \cdot \Delta_{in}} = 1 - \frac{1}{G}$$

But $G = 1/(1-f)$ from eq. (21.26). Thus

$$g = f$$

Namely, the “gain” used in some climate studies is the feedback factor used in this chapter and in electrical engineering.

HIGHER MATH • No-feedback Response

Start with no feedback, as described by the energy balance of eq. (21.31).

$$R_o = \sigma_{SB} \cdot T_e^4$$

Take the derivative:

$$dR_o = 4 \sigma_{SB} \cdot T_e^3 \cdot dT_e$$

Rearrange to find the change of output with input (dT_e/dR_o),

$$\frac{\partial T_e}{\partial R_o} = \frac{1}{4 \cdot \sigma_{SB} \cdot T_e^3}$$

Finally, convert to finite differences:

$$r_o = \frac{\Delta T_e}{\Delta R_o} = \frac{1}{4 \cdot \sigma_{SB} \cdot T_e^3} \quad (21.33)$$

Another form of this answer can be found by multiplying the numerator and denominator by T_e , and then substituting eq. (21.31) in the denominator:

$$r_o = \frac{T_e}{4 \cdot R_o}$$

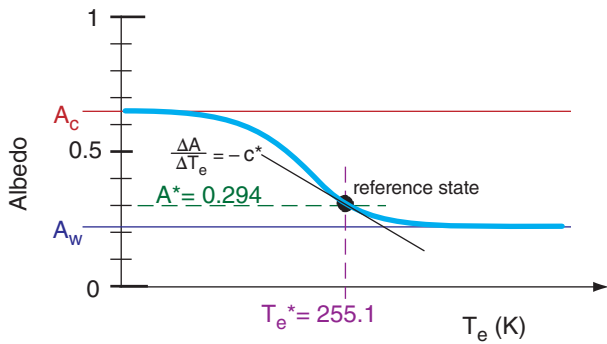


Figure 21.19
 Thick line is a sketch of response of Earth’s albedo to changes in radiative equilibrium temperature T_e , associated with changes in snow- and ice-cover. The thin line of slope $-c^*$ corresponds to the slope of the thick line at the reference point. Values for A_c and A_w are not accurate and are only for illustration.

change ΔT_e can be approximated by a straight line tangent to the curve at the reference point (Fig. 21.2), as defined by

$$r_o = \Delta T_e / \Delta R_o \tag{21.32}$$

Based on eq. (21.31), the slope r_o of this straight line (see Higher Math box on the previous page) is:

$$r_o = \frac{1}{4 \cdot \sigma_{SB} \cdot T_e^{*3}} = \frac{T_e^*}{4 \cdot R_o^*} = 0.266 \text{ K}/(\text{W}\cdot\text{m}^{-2}) \tag{21.33}$$

21.4.2.2. Ice Albedo Feedback

Next, add **ice-albedo feedback** by allowing the albedo to vary with temperature. Changes in temperature T_e alter the areal extent of highly reflective ice caps and glaciers, thereby changing the albedo (A) between two extremes (Fig. 21.19). A warm limit A_w assumes 0% snow cover, and is based on the reflectivities of the ground, crops, cities, and oceans. A cold-limit A_c represents 100% snow cover, causing a highly reflective Earth. The blackbody Earth state is useful as a reference point ($T_e^* = 255 \text{ K}$, $A^* = 0.294$).

Use the slope (thin line in Fig. 21.19) of the A vs. T_e curve at the reference point as a **linear approximation** of the nonlinear feedback (thick line). Numerical simulations of the global climate suggest this slope is:

$$\frac{\Delta A}{\Delta T} = -c^* \tag{21.34}$$

where $c^* = 0.01 \text{ K}^{-1}$. The ice-albedo feedback described here is highly oversimplified, for illustrative purposes.

For this idealized ice-albedo radiative-equilibrium case, the feedback equation (21.23) becomes:

$$\Delta T_e = r_o \cdot \Delta R_o + f \cdot \Delta T_e \tag{21.35}$$

where r_o was given in eq. (21.33), and where

$$f = \frac{c^* \cdot T_e^*}{4 \cdot (1 - A^*)} \tag{21.36}$$

(see the Higher Math box on the next page).

The resulting gain is

$$G = \frac{4 \cdot (1 - A^*)}{4 \cdot (1 - A^*) - c^* \cdot T_e^*} \tag{21.37}$$

After multiplying r_o by the gain to give r , we find that the temperature response to solar-input variations (when feedbacks ARE included) is:

$$r = \frac{(1 - A^*) \cdot T_e^*}{R_o^* \cdot [4 \cdot (1 - A^*) - c^* \cdot T_e^*]} \tag{21.38}$$

Fig. 21.20 shows how the total response r with feed-

Sample Application
 For ice-albedo radiative-equilibrium with a blackbody-Earth reference state, find the feedback factor and gain. Compare system responses with and without feedback.

Find the Answer
 Given: $T_e^* = 255 \text{ K}$, $R_o^* = 240 \text{ W}\cdot\text{m}^{-2}$, $A^* = 0.294$, $c^* = 0.01 \text{ K}^{-1}$
 Find: $r_o = ? (\text{K}/\text{W}\cdot\text{m}^{-2})$, $f = ?$, $G = ?$, $r = ? (\text{K}/\text{W}\cdot\text{m}^{-2})$

Use eq. (21.33) for the no-feedback system response:
 $r_o = (255\text{K}) / (4 \cdot 240\text{W}\cdot\text{m}^{-2}) = \underline{0.266 \text{ K}/(\text{W}\cdot\text{m}^{-2})}$

Use eq. (21.36) for the feedback factor:
 $f = (0.01 \text{ K}^{-1}) \cdot (255\text{K}) / [4 \cdot (1 - 0.294)] = \underline{0.90}$ (dim'less)

Use eq. (21.26): $G = 1 / (1 - 0.90) = \underline{10.4}$ (dimensionless)

Use eq. (21.28):
 $r = (10.4) \cdot [0.266 \text{ K}/(\text{W}\cdot\text{m}^{-2})] = \underline{2.75 \text{ K}/(\text{W}\cdot\text{m}^{-2})}$

Check: Response is reasonable. Units OK.
Exposition: This illustrates positive feedback where the response is **amplified**. For example, $\Delta S_o \approx 1 \text{ W}\cdot\text{m}^{-2}$ due to sunspot cycle (Fig. 21.11) implies $\Delta R_o = 0.175 \text{ W}\cdot\text{m}^{-2}$, giving $\Delta T_e = r \cdot \Delta R_o = 0.48^\circ\text{C}$ variation in equilibrium radiation temperature due to sunspots with feedback, compared with $\Delta T_e = 0.266^\circ\text{C}$ without.

HIGHER MATH • Feedback Example

For ice-albedo feedback, infinitesimal variations in solar irradiance dS_o and albedo dA cause infinitesimal changes in equilibrium temperature dT_e :

$$dT_e = \frac{\partial T_e}{\partial S_o} dS_o + \frac{\partial T_e}{\partial A} dA \quad (21.a)$$

To find the factors that go into this equation, start with a simple radiative-equilibrium balance:

$$T_e = \left[\frac{(1-A) \cdot S_o}{4 \cdot \sigma_{SB}} \right]^{1/4} \quad (21.3)$$

and take the derivative $\partial T_e / \partial S_o$:

$$\frac{\partial T_e}{\partial S_o} = \frac{1}{4} \left[\frac{(1-A) \cdot S_o}{4 \cdot \sigma_{SB}} \right]^{-3/4} \cdot \left[\frac{1-A}{4 \cdot \sigma_{SB}} \right]$$

Substituting eq. (21.3) into this gives:

$$\frac{\partial T_e}{\partial S_o} = \frac{1}{4} [T_e]^{-3} \cdot \left[\frac{1-A}{4 \cdot \sigma_{SB}} \right]$$

which we can rewrite as:

$$\frac{\partial T_e}{\partial S_o} = \frac{1}{4} \cdot T_e \cdot \left[\frac{1-A}{4 \cdot \sigma_{SB} \cdot T_e^4} \right]$$

Solve (21.3) for S_o and substituting into the eq. above:

$$\frac{\partial T_e}{\partial S_o} = \frac{1}{4} \cdot T_e \cdot \left[\frac{1}{S_o} \right]$$

You can similarly find $\partial T_e / \partial A$ from eq. (21.3) to be:

$$\frac{\partial T_e}{\partial A} = \frac{-T_e}{4 \cdot (1-A)}$$

When these derivatives are plugged into eq. (21.a) and applied at the reference point (S_o^* , T_e^* , A^*), the result is:

$$dT_e = \frac{T_e^*}{4 \cdot S_o^*} dS_o - \frac{T_e^*}{4 \cdot (1-A^*)} dA$$

Albedo decreases when Earth's temperature increases, due to melting snow and retreating glacier coverage:

$$dA = -c^* \cdot dT_e$$

where c^* is the magnitude of this variation at the reference point. Plugging this into the previous eq. gives:

$$dT_e = \frac{T_e^*}{4 \cdot S_o^*} dS_o + \frac{c^* \cdot T_e^*}{4 \cdot (1-A^*)} dT_e \quad (21.b)$$

(continues in next column)

HIGHER MATH • Feedback (continued)

Next, take the derivative of eq. (21.30):

$$dR_o = [(1-A)/4] \cdot dS_o$$

Dividing this by eq. (21.30) shows that:

$$\frac{dR_o}{R_o} = \frac{dS_o}{S_o}$$

Plug this into eq. (21.b), and convert from calculus to finite differences:

$$\Delta T_e = \frac{T_e^*}{4 \cdot R_o^*} \cdot \Delta R_o + \frac{c^* \cdot T_e^*}{4 \cdot (1-A^*)} \cdot \Delta T_e$$

Compare this with eq. (21.23) to realize that:

$$r_o = \frac{T_e^*}{4 \cdot R_o^*} \quad (\text{eq. 21.33}) \quad \text{and} \quad f = \frac{c^* \cdot T_e^*}{4 \cdot (1-A^*)}$$

Thus,

$$F = \frac{f}{r_o} = \frac{c^* \cdot R_o^*}{(1-A^*)} \quad \text{and} \quad G = \frac{4 \cdot (1-A^*)}{4 \cdot (1-A^*) - c^* \cdot T_e^*}$$

For the idealized (toy model) example in this section, the reference values are:

- $T_e^* = 255.1 \text{ K}$ = radiative equilibrium temperature
- $S_o^* = 1361 \text{ W}\cdot\text{m}^{-2}$ = solar irradiance
- $R_o^* = 240.2 \text{ W}\cdot\text{m}^{-2}$ = solar input / m^2 Earth's surface
- $A^* = 0.294$ (dimensionless) = albedo
- $c^* = 0.01 \text{ K}^{-1}$ = albedo response to temperature change

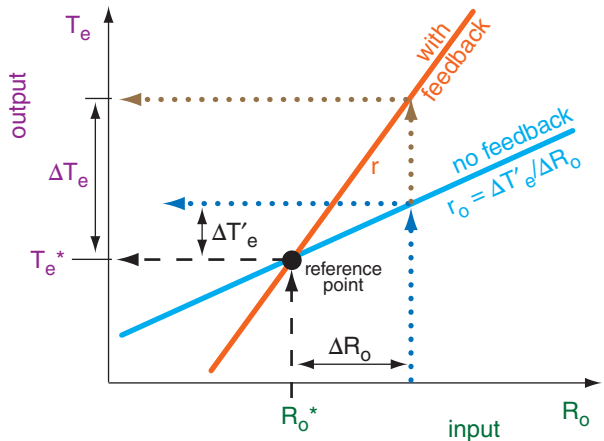


Figure 21.20
Illustration of system response with feedback (orange) and without (cyan). The prime (') denotes the no-feedback response. Different systems and feedbacks have different slopes of the response lines.

Table 21-4. Feedbacks affecting Earth’s climate.
 (+) = positive, (–) = negative feedbacks
F = Feedback parameter (W·m⁻²)·K⁻¹
f = feedback factor (dimensionless)
G = Gain (dimensionless)
r = system response K/(W·m⁻²). This is also known as the **sensitivity**, λ .

Processes for gradual climate change:				
Feedback	F	f = r ₀ F	G = 1/(1-f)	r = G·r ₀
IR Radiative (–) • blackbody Earth • realistic Earth				r ₀ = 0.27 0.31
Water-vapor (+)	1.6 ± 0.3	0.50	1.98	0.61
Lapse-rate (–)	–0.6 ± 0.4	–0.19	0.84	0.26
Cloud (+)	0.3 ± 0.7	0.09	1.1	0.34
Surface albedo (+)	0.3 ± 0.1	0.09	1.1	0.34
Ocean CO ₂ (+)				
Biological (–)				
Processes for Abrupt climate change:				
<ul style="list-style-type: none"> • Meridional Overturning Ocean Circulation • Fast Antarctic & Greenland Ice-sheet Collapse • Volcanoes • Methane Release (Hydrate Instability & Permafrost) • Biogeochemical 				

From IPCC, AR5, 2013, Chapter 9, Table 9.5 & Fig. 9.43.

Sample Application

Given the feedbacks listed in Table 21-4, what is the total response.

Find the Answer

Given: Table 21-4. Use realistic Earth for r₀.
 Find: r = ? K/(W·m⁻²).
 Assume: total response is based on only those feedback processes for which numbers are given in the table.

Use eq. (21.29): $G = 1 / [1 - \Sigma f]$
 $G = 1 / [1 - (0.50 - 0.19 + 0.09 + 0.09)]$
 $G = 1 / [1 - 0.49] = 1.96$

Use eq. (21.28): $r = G \cdot r_0$
 $r = 1.96 \cdot 0.31 = \underline{0.61} \text{ K/(W·m}^{-2}\text{)}$.

Check: Units OK. Physics OK.

Exposition: For each $\Delta R = 1 \text{ W·m}^{-2}$ change in solar input, the Earth-system response with all feedbacks is $\Delta T = 0.61 \text{ K}$, which is twice the response (0.31 K) without feedback (other than the background IR feedback). {CAUTION: The total response is NOT equal to the sum of the individual responses *r*. Instead, use the sum of feedback factors *f* to get the net feedback.}

back differs from the r₀ without. With feedback, eq. (21.32) becomes:

$$\Delta T_e = r \cdot \Delta R_0 \tag{21.39}$$

Table 21-4 lists some feedbacks that can affect Earth’s climate. These are briefly discussed next.

21.4.3. Infrared Radiative (IR) Feedback

IR is the strongest feedback — it dominates all others. It was already discussed as the “radiation out” term in eq. (21.2). This important negative (–) feedback allows the Earth to have an equilibrium state. Even a small change in Earth’s temperature results in a strong compensating energy loss because IR radiation is proportional to the 4th power of T_e in the Stefan-Boltzmann equation. This strong damping keeps Earth’s climate relatively steady.

As we have seen, the reference black-body response to changes in net solar input is r₀ = 0.267 K/(W·m⁻²). Global climate models that include more realistic atmospheric absorption and emission of IR radiation find r₀ = 0.31 ± 0.01 K/(W·m⁻²).

21.4.4. Water-vapor Feedback

Warmer air can hold more water vapor, which absorbs and re-radiates more IR radiation back to the surface and reduces the atmospheric window sketched in Fig. 21.5. The warmer surface warms the air, resulting in a very strong positive feedback (see Table 21-4). The upper troposphere is where this feedback is most effective.

Water vapor is an important natural greenhouse gas. If the climate warms and the upper tropospheric water-vapor content increases to the point where the atmospheric window is mostly closed (net atmospheric emissivity e ≈ 1), then we return to the negative feedback sketched in Fig. 21.4 and steady Earth temperature of T_s = 30°C from eq. (21.6).

21.4.5. Lapse-rate Feedback

The simple model of Fig. 21.4 uses the same air temperature T_A to determine IR radiation both up to space and down toward the Earth. However, in the real atmosphere the temperature decreases with an average lapse rate 6.5 °C·km⁻¹ in the troposphere. Thus, colder temperatures at the top of the troposphere emit less upward IR radiation to space than is emitted downward from the warmer bottom of the troposphere. This difference in upward and downward IR radiation is part of our normal climate, causing our normal temperatures.

Global warming tends to reduce the lapse rate. Namely, the temperature difference diminishes between the top and bottom of the troposphere. Rel-

ative to each other, IR radiation out to space will increase and IR radiation down toward the Earth will decrease. The net effect is to cool the Earth system. Thus, lapse-rate feedback is negative (Table 21-4).

Water-vapor and lapse-rate feedbacks are closely related, and are often considered together. Their combined effect is a modest positive feedback.

21.4.6. Cloud Feedback

Cloud feedback is likely important, but the details are poorly understood. Relative to clear skies, clouds at all heights cause cooling by reflecting incoming solar radiation. But clouds also cause warming by trapping (absorbing and re-radiating back towards the surface) upwelling IR radiation. The small difference between these large opposing forcings can have very large error, depending on cloud type and altitude. For our present climate, the net effect of clouds is cooling.

Table 21-4 indicates a positive feedback for clouds, based on global climate modeling. Namely, an increase in radiative input to the Earth system would decrease the cloud cover, thus causing less cooling. But much more research must be done to gain more confidence in cloud-feedback processes.

Sometimes **aerosol feedback** is grouped with cloud feedback. Aerosols (microscopic solid or liquid particles in the air) can have similar effects as cloud droplets. However, some aerosols such as sulfates are darker than pure water droplets, and can absorb more solar radiation to cause atmospheric warming. As already discussed, volcanoes can inject sulfate aerosols into the stratosphere. **Phytoplankton** (microscopic plant life) in the ocean can release into the atmospheric boundary layer a chemical called dimethyl sulfide, which can later be oxidized into sulfate aerosols.

21.4.7. Ice–albedo (Surface) Feedback

This positive feedback was discussed earlier in the idealized feedback example, where we found a response of $r = 2.75 \text{ K}/(\text{W}\cdot\text{m}^{-2})$ in the Sample Application. More realistic estimates from Global Climate Model simulations are $r = 0.27$ to $2.97 \text{ K}/(\text{W}\cdot\text{m}^{-2})$. At our current reference temperature, this feedback mostly affects the climate at high latitudes.

This positive-feedback sensitivity applies only over the limited range of Fig. 21.19 for which albedo can vary with temperature. At the cold extreme of a completely snow-covered Earth (**snowball Earth**), the albedo is constant at its cold-limit value A_c . At the warm extreme the Earth has no ice caps or snow cover, and albedo is constant at A_w .

At these two extremes, the negative feedback of IR radiation again dominates, leading to steady

Sample Application

Use Table 21-4 to estimate the combined water-vapor and lapse-rate response, $r_{wv.lr}$.

Find the Answer

Given Table 21-4: $f_{water.vapor} = 0.50$, $f_{lapse.rate} = -0.19$

Find: $r_{wv.lr} = ? \text{ K}/(\text{W}\cdot\text{m}^{-2})$

Assume: $r_o = 0.31 \text{ K}/(\text{W}\cdot\text{m}^{-2})$ for a realistic Earth.

For multiple feedbacks, we must use eq. (21.29):

$$G = 1 / [1 - (0.50 - 0.19)] = 1.45$$

Use eq. (21.28):

$$r_{wv.lr} = 1.45 \cdot [0.31 \text{ K}/(\text{W}\cdot\text{m}^{-2})] = \mathbf{0.45 \text{ K}/(\text{W}\cdot\text{m}^{-2})}$$

Check: Units OK. Magnitude OK.

Exposition: This r corresponds to $G = 1.45$, $f = 0.311$, & $F = 1.003$, which agrees with IPCC AR5 Fig. 9.43.

INFO • Greenhouse Gases

A **greenhouse gas (GHG)** is an atmospheric gas that absorbs and emits IR radiation. Of particular concern are gases that absorb and emit within the 8 to 14 μm wavelength range of the **atmospheric window**. As the concentrations of such gases increase, the atmospheric window can close due to the increased atmospheric emissivity (Fig. 21.5), resulting in global warming.

Greenhouse gases, ranked by importance, are:

- (1) water vapor (H_2O),
- (2) carbon dioxide (CO_2),
- (3) methane (CH_4),
- (4) nitrous oxide (N_2O),
- (5) ozone (O_3),
- (6) halocarbons [e.g., freon CFC-12 ($\text{C Cl}_2 \text{ F}_2$)]

Except for (6), most greenhouse gases have both natural and **anthropogenic** (man-made) sources. CO_2 is of particular concern because it is released by humans burning fossil fuels (coal, oil) for energy.

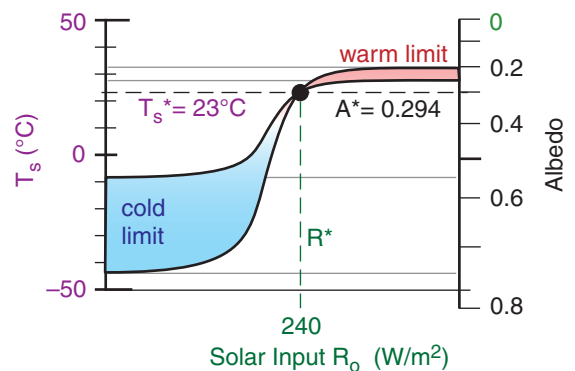


Figure 21.21

Illustration of how Earth’s surface temperature is bounded once the Earth becomes fully snow-covered (cold limit) or fully snow-free (warm limit). Shading shows temperature uncertainty due to uncertainty in the limiting albedo values.

INFO • Climate Sensitivity

The Intergovernmental Panel on Climate Change (IPCC) states that **climate sensitivity** is “a measure of the climate system response to sustained radiative forcing. It is defined as the equilibrium global average surface warming” (ΔT_s) “following a doubling of CO₂ concentration.”

Based on research by international teams using global climate models, IPCC suggests in their 5th Assessment Report (AR5, 2013) that “this sensitivity is likely to be in the range of” $\Delta T_s =$ “1.5 to 4.5°C with a best estimate of 3.2°C” for a doubling of the greenhouse gas CO₂. This temperature rise would be equivalent to a **radiative forcing** (ΔR_o in Fig. 21.18b' & c'; abbreviated as **RF** by IPCC) of $3.4 \pm 0.8 \text{ W}\cdot\text{m}^{-2}$.

CO₂ has not doubled yet, but since year 1700 the concentration increased from 275 to 410 ppm (Fig. 21.k).

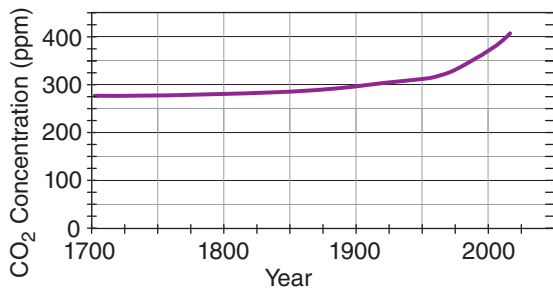


Fig 21.k. Keeling curve, based on ice-core data before 1958, and Mauna Loa data after. The shape of the curve looks somewhat like a **hockey stick**. [Based on data from <https://scripps.ucsd.edu/programs/keelingcurve/>.]

IPCC is particularly concerned about anthropogenic forcings, because these can be mitigated by people. Since year 1750 — the start of the industrial age — people have inadvertently altered the Earth-system net radiative forcing as follows (IPCC AR5 Table 8.6):

Anthropogenic Process	ΔR_o or RF (W·m⁻²)
Well-mixed greenhouse gases (CO ₂ + CH ₄ + N ₂ O + Halocarbons)	+2.83
O ₃ in stratosphere	-0.05
O ₃ in troposphere	0.40
H ₂ O from CH ₄ in stratosphere	0.07
Surface albedo/land use	-0.15
Surface albedo/carbon on snow	0.04
Aerosols/ direct	-0.35
Jet contrails	+0.01

Total Anthropogenic (was not estimated in the AR5 report) in AR4 was estimated as **+1.6** range [0.6 to 2.4]

Compare this to a natural process:

Solar irradiance change **+0.05**

The large anthropogenic effects relative to the natural solar variations is what motivates policy makers to take action.

Earth temperatures. For snowball Earth, cold-limit albedo estimates are in the range of $0.55 \leq A_c \leq 0.75$. When used in the radiation balance of eq. (21.3) the cold-limit blackbody temperature is $197 \text{ K} \leq T_e \leq 228 \text{ K}$, yielding a surface temperature ($T_s = 1.161 \cdot T_e$, from eq 21.10) of $-44^\circ\text{C} \leq T_s \leq -8^\circ\text{C}$.

For the warm limit (assuming that clouds having 37% albedo still cover roughly 70% of the Earth) $0.20 \leq A_w \leq 0.25$, and the equilibrium blackbody temperature is $259 \text{ K} \leq T_e \leq 263 \text{ K}$. This corresponds to a surface temperature of $28^\circ\text{C} \leq T_s \leq 33^\circ\text{C}$ using eq. (21.10). Thus, runaway global warming or cooling is not possible beyond these bounds (see Fig. 21.21).

21.4.8. Ocean CO₂ Feedback

Warmer seawater can hold less dissolved carbon dioxide (CO₂) than colder water (see INFO box on next page). Hence global warming will cause oceans to release CO₂ into the atmosphere. Greater atmospheric CO₂ concentrations reduce the atmospheric window due to an increase in net atmospheric emissivity e , and thus cause the atmosphere to re-radiate more IR radiation back toward the Earth surface. The net result is positive feedback.

21.4.9. Biological CO₂ Feedback

As plants grow, they consume CO₂ to make hydrocarbons and carbohydrates via photosynthesis. As a result, the carbon is **sequestered** (stored) as the body of the plant. Some of the carbohydrates (e.g., sugars) are consumed by the plant, and are converted back to CO₂ and **transpired** (exhaled by the plant) into the atmosphere.

When plants die and decay, or when they burn in a **wild fire**, they release their remaining carbon as CO₂ back to the atmosphere. If plants are buried under sediment before they decay or burn, their carbon can be fossilized into coal, oil, natural gas (**fossil fuels**). Carbonate rocks can also sequester carbon from the atmosphere, but the carbon can later be released through weathering of the rocks.

The change of carbon from CO₂ to other forms is called the **global carbon cycle**. It is extremely difficult to model the global carbon cycle, which leads to large uncertainty in estimates of climate feedback. Also, anthropogenic effects of fossil-fuel and biomass burning affect the cycle. At present, it is believed that biological CO₂ causes a positive feedback. Namely, global warming will cause more CO₂ to be released than sequestered.

Processes of **abrupt climate change** in Table 21-4 are left to the reader to explore (via an Evaluate & Analyze exercise).

21.5. GAIA HYPOTHESIS & DAISYWORLD

James Lovelock proposed a thought-provoking hypothesis: life regulates the climate to create an environment that favors life. Such self-maintained stability is called **homeostasis**. His hypothesis is called **gaia** — Greek for “mother Earth”.

Lovelock and Andrew Watson illustrate the “biological homeostasis of the global environment” with **daisyworld**, a hypothetical Earth containing only light and dark colored daisies. If the Earth is too cold, the dark daisies proliferate, increasing the absorption of solar radiation. If too warm, light-colored daisies proliferate, reflecting more sunlight by increasing the global albedo (Fig. 21.22).

21.5.1. Physical Approximations

We modify Lovelock’s toy model here to enable an easy solution of daisyworld on a spreadsheet. Given are two constants: the Stefan-Boltzmann constant $\sigma_{SB} = 5.67 \times 10^{-8} \text{ W}\cdot\text{m}^{-2}\cdot\text{K}^{-4}$ and solar irradiance $S_0 = 1361 \text{ W}\cdot\text{m}^{-2}$. Small variations in solar output are parameterized by luminosity, L , where $L = 1$ corresponds to the actual value for Earth. These factors are combined into a solar-forcing ratio, q :

$$q = \frac{L \cdot S_0}{4 \cdot \sigma_{SB}} \tag{21.40}$$

The model forecasts the fraction of the globe covered by light daisies (C_L) and the fraction covered by dark daisies (C_D). Some locations will have no daisies, so the bare-ground fraction (C_G) of Earth’s surface is thus:

$$C_G = 1 - C_D - C_L \tag{21.41}$$

To start the calculation, assume an initial state of $C_L = C_D = 0$.

Define a planetary albedo (A) as the coverage-weighted average of the individual daisy albedoes (A_i , which are adjustable parameters):

$$A = C_G \cdot A_G + C_D \cdot A_D + C_L \cdot A_L \tag{21.42}$$

For this example, let:

- $A_L = 0.75$ is the albedo of light-colored daisies
- $A_D = 0.25$ is the albedo of dark-colored daisies
- $A_G = 0.5$ is the bare-ground albedo (no flowers).

Use the planetary albedo with the solar forcing ratio to find daisyworld’s effective-radiation absolute temperature:

$$T_e^4 = q \cdot (1 - A) \tag{21.43}$$

INFO • Effervescence and CO₂

Carbonated beverages retain their tart flavor when cold. The tartness or sourness comes from carbonic acid (H₂CO₃) due to CO₂ dissolved in water (H₂O). But as the beverage warms, it cannot hold as much dissolved CO₂, forcing some of the CO₂ to **effervesce** (bubble out). Namely, the beverage loses its fizz, causing it to taste “flat”.

The same phenomenon happens to the oceans. If oceans warm, they lose some of their fizz.

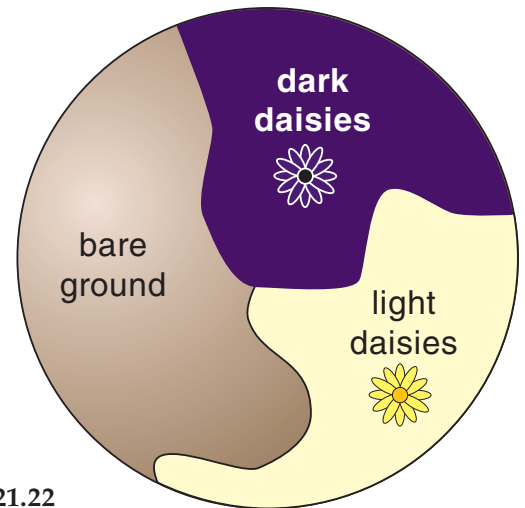


Figure 21.22
A hypothetical daisyworld with only light and dark colored flowers and bare ground.

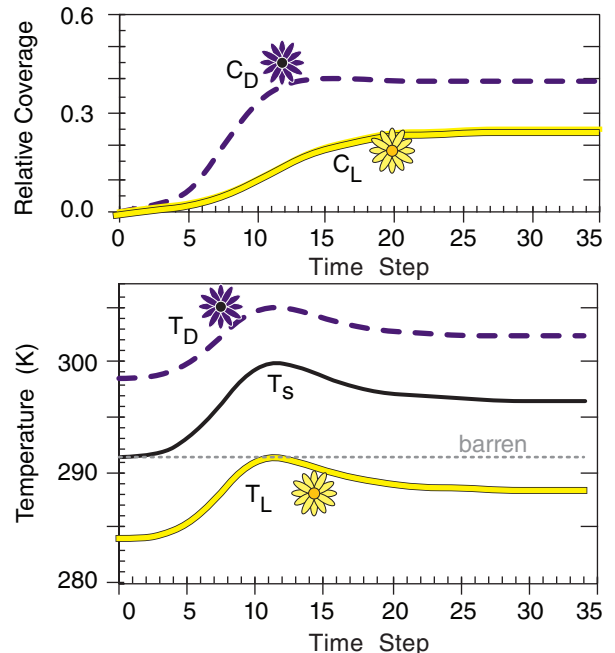


Figure 21.23
Evolution of daisy coverage and temperatures as daisyworld evolves toward an equilibrium, given a luminosity of $L = 1.2$.

Sample Application (\$)

Compute and plot the evolution of temperatures and daisy coverage for a daisyworld having: bare ground albedo = 0.45, light-colored daisy albedo = 0.85, dark daisy albedo = 0.2, daisy death rate = 0.25, transport parameter = 0.65, luminosity of the sun = 1.5, seed coverage = 0.01, and time step = 0.5 .

Find the Answer

Given: $D=0.25$, $A_L=0.85$, $A_D=0.20$, $A_G=0.45$,
 $Tr=0.65$, $L=1.5$, $C_s = 0.01$
 Find: $T_L = ?$ K, $T_D = ?$ K, $T_s = ?$ K, $C_L = ?$, $C_D = ?$

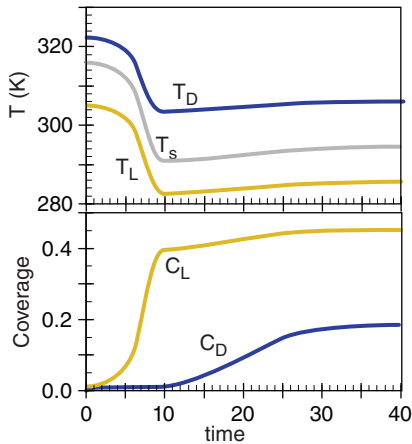
Find the solar forcing ratio from eq. (21.40):

$$q = \frac{1.5 \cdot (1361 \text{ W} \cdot \text{m}^{-2})}{4 \cdot (5.67 \times 10^{-8} \text{ W} \cdot \text{m}^{-2} \cdot \text{K}^{-4})} = 9.003 \times 10^9 \text{ K}^4$$

Because we are not told an initial coverage of daisies, assume $C_L = C_D = 0$.

Use eqs. (21.41 - 21.46) in a spreadsheet, and iterate forward in time from $t = 0$ using $\Delta t = 0.5$.

t	C_D	C_L	C_G	A	T_s (K)	T_D (K)	T_L (K)	β_D	β_L
0	0.00	0.00	1.00	0.45	315.4	321.5	304.8	0.00	0.71
0.5	0.01	0.01	0.98	0.45	315.2	321.3	304.7	0.00	0.73
1	0.01	0.01	0.98	0.45	315.1	321.2	304.5	0.00	0.73
1.5	0.01	0.02	0.97	0.45	314.9	321.1	304.4	0.00	0.74
2	0.01	0.02	0.97	0.45	314.7	320.9	304.2	0.00	0.75
...									
7	0.01	0.20	0.79	0.53	303.4	312.3	293.9	0.08	0.99
7.5	0.01	0.26	0.73	0.55	299.8	309.6	290.7	0.35	0.92
...									
36.5	0.18	0.45	0.37	0.58	294.1	305.4	285.5	0.68	0.68
37	0.18	0.45	0.37	0.58	294.1	305.4	285.5	0.68	0.68



Check: Physics & units are OK.

Exposition: The solar luminosity is large, causing a planetary temperature that is initially too warm for any dark-colored daisies (except for the seed coverage). But as light-colored daisies proliferate, the world cools to the point where some dark-colored daisies can grow. The final steady surface temperature is not very different from that on the previous page, even though this world has more light than dark daisies.

For a one-layer atmosphere with no window, the average surface temperature is

$$T_s^4 = 2 \cdot T_e^4 \tag{21.44}$$

Let $Tr = 0.6$ be an efficiency for horizontal heat transport. For example, $Tr = 1$ implies efficient spreading of heat around the globe, causing the local temperature to be controlled by the global-average albedo. Conversely, $Tr = 0$ forces the local temperature to be a function of only the local albedo in any one patch of daisies.

Thus, the patches of dark and light daisies have the following temperatures:

$$T_D^4 = (1 - Tr) \cdot q \cdot (A - A_D) + T_s^4 \tag{21.45a}$$

$$T_L^4 = (1 - Tr) \cdot q \cdot (A - A_L) + T_s^4 \tag{21.45b}$$

Suppose that daisies grow only if their patch temperatures are between 5°C and 40°C, and that daisies have the fastest growth rate (β) near the middle of this range (where $T_0 = 295.5 \text{ K} = 22.5^\circ\text{C}$):

$$\beta_D = 1 - b \cdot (T_0 - T_D)^2 \tag{21.46a}$$

$$\beta_L = 1 - b \cdot (T_0 - T_L)^2 \tag{21.46b}$$

where negative values of β are truncated to zero. The growth factor is $b = 0.003265 \text{ K}^{-2}$.

Because dark and light daisies interact via their change on the global surface temperature, you must iterate the coverage equations together as you step forward in time

$$C_{D \text{ new}} = C_D + \Delta t \cdot C_D \cdot (C_G \cdot \beta_D - D) \tag{21.47a}$$

$$C_{L \text{ new}} = C_L + \Delta t \cdot C_L \cdot (C_G \cdot \beta_L - D) \tag{21.47b}$$

where $D = 0.3$ is death rate (another adjustable parameter) for both light and dark daisies. In this iteration, the daisy coverages (C_D & C_L) at any one time step can be inserted into the right side of the above two equations, and the solution can be stepped forward in time to find the new coverages ($C_{D \text{ new}}$ & $C_{L \text{ new}}$) one time step Δt later. The time units are arbitrary, so you could use $\Delta t = 1$ or $\Delta t = 0.5$. To get daisies to grow if none are on the planet initially, assume a seed coverage of $C_s = 0.01$ and force $C_{L \text{ new}} \geq C_s$ and $C_{D \text{ new}} \geq C_s$.

With the new coverages, eqs. (21.41 - 21.47) can be computed again for the next time step. Repeat for many time steps. For certain values of the parameters, the solution (i.e., coverages and temperatures) approaches a steady-state, which results in the desired homeostasis equilibrium.

21.5.2. Steady-state and Homeostasis

Suppose $L = 1.2$ with all other parameters set as described in the Physical Approximations subsection. After iterating, the final steady-state values are $C_L = 0.24$, $C_D = 0.40$ and $T_s = 296.8$ K (see Fig. 21.23). Compare this to the surface temperature of a planet with no daisies: $T_{s \text{ barren}} = 291.3$ K, found by setting $A = A_G$ in eqs. (21.43 - 21.44).

Suppose you rerun daisyworld with all the same parameters, but with different luminosity. The resulting steady-state conditions are shown in Fig. 21.24 for a variety of luminosities. For luminosities between about 0.94 to 1.70, the daisy coverage is able to adjust so as to maintain a somewhat constant T_s — namely, it achieves homeostasis. Weak incoming solar radiation (insolation) allows dark daisies to proliferate, which convert most of the insolation into heat. Strong insolation is compensated by increases in light daisies, which reflect the excess energy.

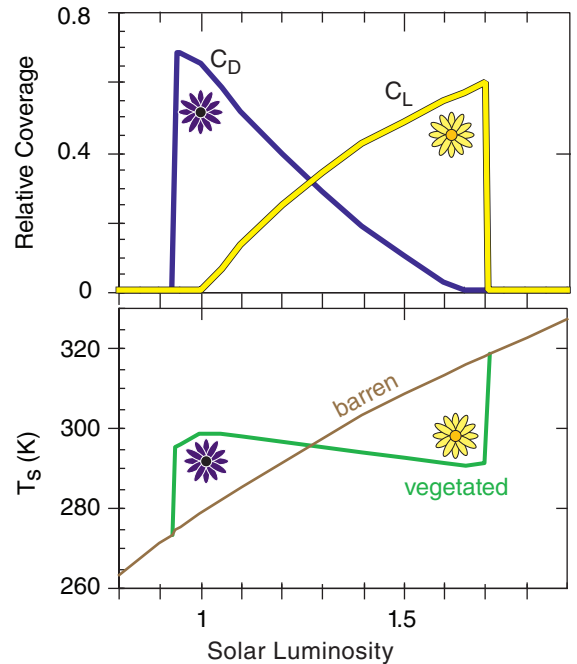


Figure 21.24

Final steady-state values of average surface temperature T_s and daisy coverages (C_D & C_L), as a function of luminosity. The bottom graph compares the lushly flowered (vegetated) world with an unflowered (barren) world.

21.6. GCMS

Some computer codes for numerical weather prediction (see the NWP chapter) are designed to forecast global climate. These codes, called **GCMs** (global climate models) have a somewhat-coarse 3-D arrangement of grid points filling the global atmosphere. At each grid point the governing equations for heat, momentum, mass, moisture, and various chemicals are repeatedly solved as the GCM iterates forward in time.

Other GCMs use spectral rather than grid-point numerics in the horizontal, where a sum of sine waves of various wavelengths are used to approximate the spatial structure of the climate. Regardless of the numerical scheme, the GCM is designed to forecast decades or even centuries into the future.

Such a long-duration forecast is computationally expensive. Improved climate forecasts are possible by coupling forecasts of the atmosphere, ocean, biosphere, cryosphere (ice) and soil — but this further increases computational expense. To speed up the forecast, compromises are made in the numerics (e.g., coarse grid spacing in the horizontal; reduced number of vertical layers), dynamics, or physics (e.g., simplified parameterizations of various feedbacks).

One disadvantage of coarse grid spacings is that some dynamical and physical phenomena (e.g., thunderstorms, thermals, clouds, etc.) become **subgrid scale**, meaning they are not directly resolvable. As an example, a GCM with horizontal grid spacing of 1° of latitude would be able to resolve phenomena as small as 7° of latitude (≈ 777 km); hence, it could not “see” individual thunderstorms or clusters of thun-

Human- & Climate-Change Timescales

“We tend to predict impacts on people by assuming a static human society. But humans are adapting quickly, and time scales of human change are faster than the climate change. There’s no unique perfect temperature at which human societies operate. Run them a little warmer, and they’ll be fine; run them a little cooler, they’ll be fine. People are like roaches — hard to kill. And our technology is changing rapidly, and we’re getting richer, internationally and individually, at an absurd rate. We’re rapidly getting less and less sensitive to climatic variations.”

— David Keith
(from an interview published in *Discover*, Sep 2005.)

Table 21-5. Both OPMs (Operational Prognostic Models, for short-range daily forecasts) and GCMs (Global Climate Models, for long-range simulations) are NWP (Numerical Weather Prediction) models.

Characteristic	OPM	GCM
desired outcome	deterministic forecasts (of the actual weather)	forecasts that are statistically skillful (e.g., forecast the right number of cyclones, even though their locations and times are wrong)
forecast horizon	days	decades
horizontal grid spacing	10 m to 10 km	10 km to 100 km
boundary conditions	less important	more important
initial conditions	very important	less important
approximations	partially parameterized	extensively parameterized

derstorms. Although unresolved, subgrid-scale thunderstorms still affect the global climate forecast. Therefore their effects must be approximated via **parameterizations**.

Even for resolvable phenomena such as midlatitude cyclones, GCMs are designed to forecast the correct number of cyclones, although their locations and dates are usually incorrect (Table 21-5). The motivation is that the correct number of cyclones will transport the correct amount of heat, moisture and momentum when averaged over long time periods, thus increasing the likelihood that the climate simulation is reasonable.

Other phenomena, such as solar input or deep-soil temperatures, are imposed as boundary conditions (BCs). By very careful prescription of these BCs, the GCM can be designed so that its numerical climate does not drift too far from the actual climate. This is often validated by running the GCM for past years and comparing the result to the observed climate, giving confidence that the same accuracy is possible for future years.

Initial conditions (ICs) are less important for GCMs, because the ability to forecast the exact location of individual cyclones decreases to nil within a week or so (see the Forces and Winds Chapter).

GCMs are often used to address what-if questions, such as “what if the concentration of CO₂ were to double”, or “what if deforestation were to reduce vegetation coverage.” By comparing GCM runs with and without CO₂ doubling or deforestation, we can estimate the effects of such changes on future climate. But such predictions carry a lot of uncertainty because of the many parameterizations and approximations used in GCMs.

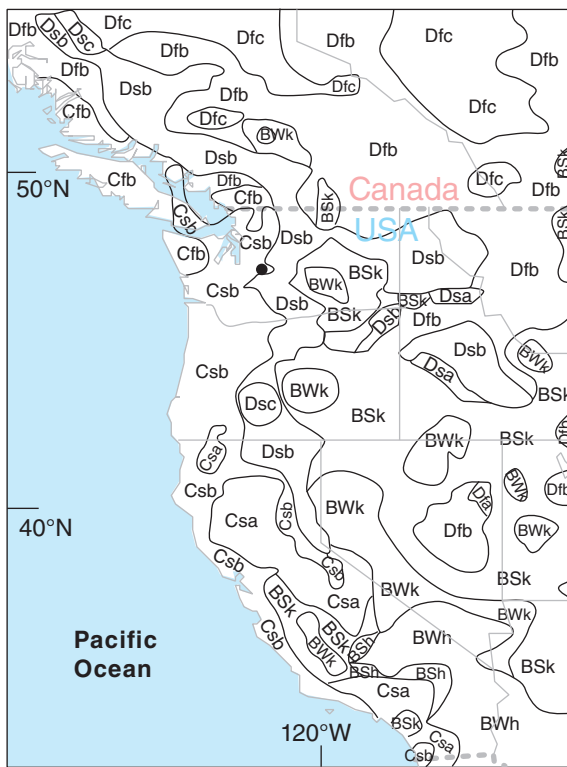


Figure 21.25
Köppen climate map for western North America. See Tables 21-6 & 21-8 for explanations of the climate code letters. [Color maps of Köppen climate classification for the whole world are available on the internet.]

21.7. PRESENT CLIMATE

So far, we have focused on processes that create and modify global climate. But before we leave this chapter, let’s briefly summarize current climate.

21.7.1. Definition

Climate describes the slowly varying characteristics of the atmosphere, as part of the atmosphere/hydrosphere/cryosphere/biosphere/land-surface system. Climate is found by averaging or filtering the hourly or daily weather data over 30 years, with the last year ending in zero (e.g., 1981-2010, or 1991-2020). Mean values of weather, temporal and spatial variability, and extremes are the statistics that are recorded as components of the climate signal.

Table 21-6. Köppen climate codes and defining criteria. (Peel et al, 2007). Also see Table 21-8 near end of chapter.

1 st	2 nd	3 rd	Description	Criteria* (see footnotes below)
A			Tropical	$T_{cold} \geq 18$
	f m w		Rainforest Monsoon Savannah	$P_{dry} \geq 60$ [not Af] and $[P_{dry} \geq (100 - MAP/25)]$ [not Af] and $[P_{dry} < (100 - MAP/25)]$
B			Arid	$MAP < [10 \cdot P_{threshold}]$
	W S		Desert Steppe	$MAP < [5 \cdot P_{threshold}]$ $MAP \geq [5 \cdot P_{threshold}]$
		h k	Hot Cold	$MAT \geq 18$ $MAT < 18$
C			Temperate	$[T_{hot} \geq 10]$ and $[0 < T_{cold} < 18]$
	s w f		Dry summer Dry winter Without dry season	$[P_{sdry} < 40]$ and $[P_{sdry} < (P_{wwet}/3)]$ $P_{wdry} < [P_{swet}/10]$ [not Cs] and [not Cw]
		a b c	Hot summer Warm summer Cold summer	$T_{hot} > 22$ [not a] and $[N_{monT10} \geq 4]$ [not (a or b)] and $[1 \leq N_{monT10} < 4]$
D			Cold	$[T_{cold} \leq 0]$ and $[T_{hot} > 10]$
	s w f		Dry summer Dry winter Without dry season	$[P_{sdry} < 40]$ and $[P_{sdry} < (P_{wwet}/3)]$ $P_{wdry} < [P_{swet}/10]$ [not Ds] and [not Dw]
		a b c d	Hot summer Warm summer Cold summer Very cold winter	$T_{hot} \geq 22$ [not a] and $[T_{mon10} \geq 4]$ [not (a or b or d)] [not (a or b)] and $T_{cold} < -38$
E			Polar	$T_{hot} < 10$
	T F		Tundra Frost	$T_{hot} > 0$ $T_{hot} \leq 0$

21.7.2. Köppen Climate Classification

In 1884, Wladimir Köppen used temperature and precipitation to define different types of climate. He drew maps, classifying every point on land according to these climates. The climate at each location controls the dominant type of plants that naturally grow there. The Köppen climate map was modified by Rudolf Geiger in the early 1900s, and was significantly updated in 2007 by Peel, Finlayson and McMahon (*Hydrol. Earth Syst. Sci.*, **11**, 1633-1644) using modern weather data.

A two- or three-letter code is used to identify each climate type (also see Table 21-8 in the Homework Exercises section). The criteria used to classify the climate types are detailed in Table 21-6. Fig. 21.25 shows a small portion of the global climate map.

Table 21-6 (continuation). *Footnotes

MAP	= mean annual precipitation (mm·yr ⁻¹)
MAT	= mean annual temperature (°C)
N_{monT10}	= number of months where the temperature is above 10 (°C)
P_{dry}	= precipitation of the driest month (mm·month ⁻¹)
P_{sdry}	= precipitation of the driest month in summer (mm·month ⁻¹)
P_{swet}	= precipitation of the wettest month in summer (mm·month ⁻¹)
P_{wdry}	= precipitation of the driest month in winter (mm·month ⁻¹)
P_{wwet}	= precipitation of the wettest month in winter (mm/month)
T_{hot}	= average temperature of the hottest month (°C)
T_{cold}	= average temperature of the coldest month (°C)
$P_{threshold}$ (mm)	= is given by the following rules: If ($\geq 70\%$ of MAP occurs in winter) then $P_{threshold} = (2 \cdot MAT)$ Else if ($\geq 70\%$ of MAP occurs in summer) then $P_{threshold} = (2 \cdot MAT) + 28$ Else $P_{threshold} = (2 \cdot MAT) + 14$
Summer (winter) is defined as the warmer (cooler) six month period of [1 Oct. - 31 Mar.] and [1 Apr. - 30 Sep.].	

Table 21-7. Climate oscillations. SST = sea-surface temperature, SLP = sea-level pressure.

Name	Period (yr)	Key Place	Key Variable
El Niño (EN)	2 to 7	Tropical E. Pacific	SST
Southern Oscillation (SO)	2 to 7	Tropical Pacific	SLP
Pacific Decadal Oscillation (PDO)	20 to 30	Extratrop. NE Pacific	SST
North Atlantic Oscillation (NAO)	variable	Extratrop. N. Atlantic	SLP
Arctic Oscillation (AO)	variable	N. half of N. hem.	SLP
Madden-Julian Oscillation (MJO)	30 to 60 days	Tropical Indian & Pacific	Convective Precipitation

INFO • What is an Oscillation?

Oscillations are regular, repeated variations of a measurable quantity such as temperature (T) in space x and/or time t . They can be described by sine waves: $T = A \cdot \sin[C \cdot (t - t_0) / \tau]$ where A is a constant **amplitude** (signal strength), τ is a constant **period** (duration one oscillation), t_0 is a constant **phase shift** (the time delay after $t = 0$ for the signal to first have a positive value), and C is 2π radians or 360° (depending on your calculator).

True oscillations are **deterministic** — the signal T can be predicted **exactly** for **any** time in the future. The climate “oscillations” discussed here are not deterministic, cannot be predicted far in the future, and do not have constant amplitude, period, or phase.

21.8. NATURAL OSCILLATIONS

The 30-year-average climate is called the **normal climate**. Any shorter-term (e.g., monthly) average weather that differs or varies from the climate norm is called an **anomaly**. Natural climate “oscillations” are recurring, multi-year anomalies with irregular amplitude and period, and hence are not true oscillations (see the INFO Box).

Table 21-7 lists some of these oscillations and their major characteristics. Although each oscillation is associated with, or defined by, a location or place on Earth (Fig. 21.26), most of these oscillations affect climate over the whole world. At the defining place(s), a combination of key weather variables is used to define an “**index**”, which is the varying climate signal. Fig. 21.27 shows some of these oscillation indices.

21.8.1. El Niño - Southern Oscillation (ENSO)

El Niño (La Niña) occurs when the tropical sea-surface temperature (SST) in the central and eastern Pacific ocean is warmer (cooler) than the multi-decadal climate average.

The El Niño index plotted in Fig. 21.27a is the Pacific SST anomaly in the tropics (Niño region 3.4, averaged within $\pm 5^\circ$ latitude of the equator, between $170 - 120^\circ$ West) minus the Pacific SST anomaly outside the tropics (averaged over more poleward latitudes). Alternative El Niño indices are also useful.

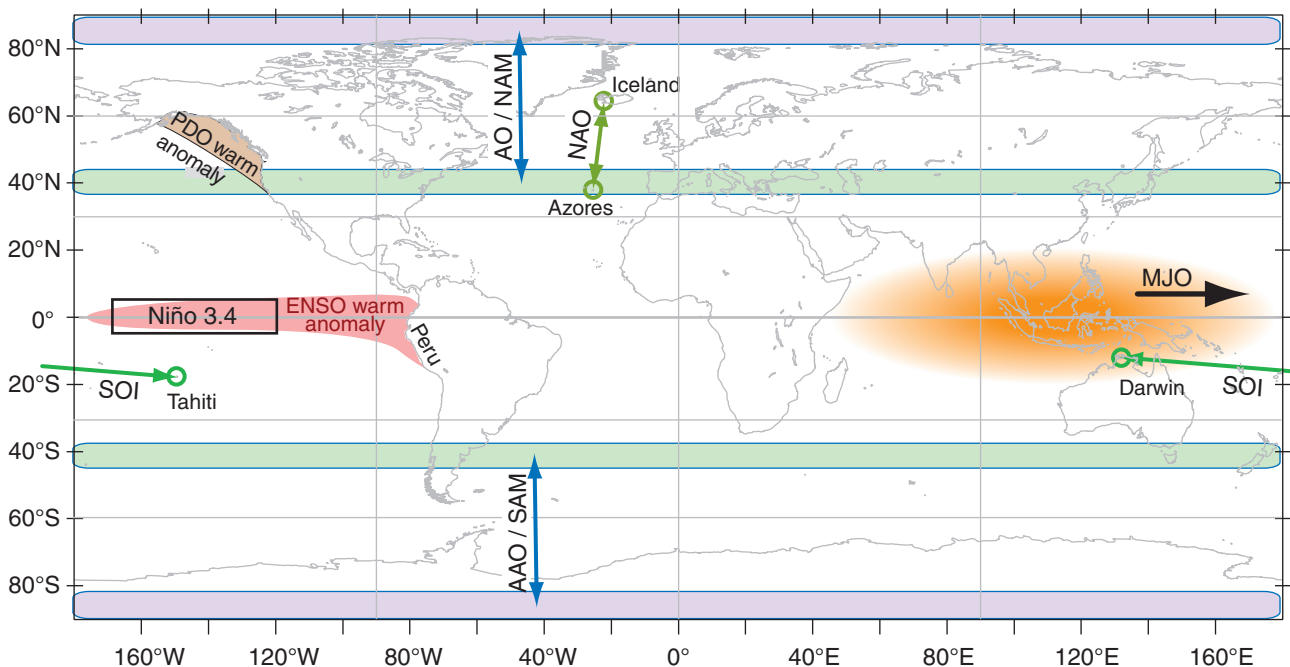


Figure 21.26 Places and key variables that define some climate oscillations. Acronyms are defined in the text.

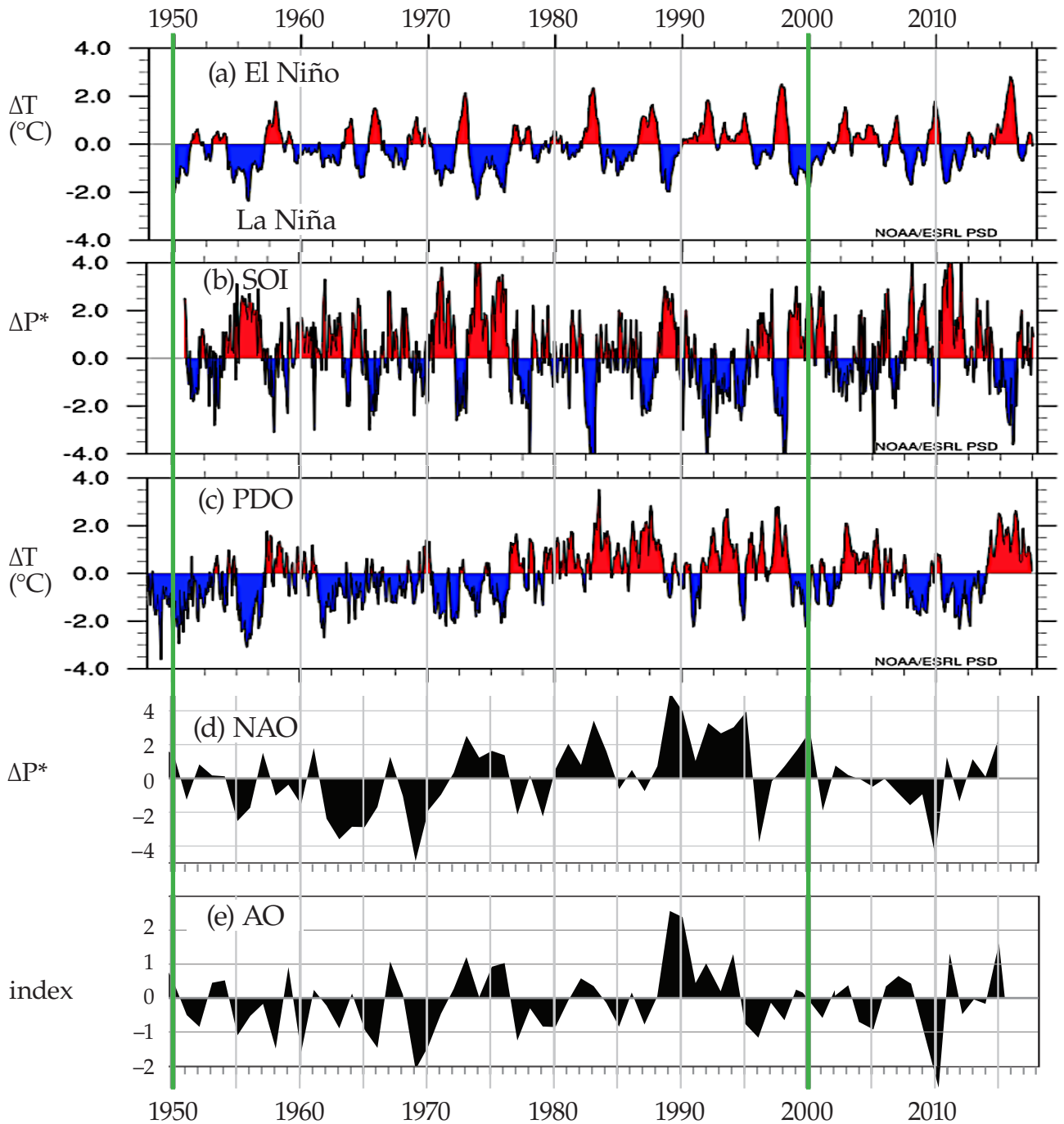


Figure 21.27

Natural oscillations of some climate indices.

- (a) **El Niño 3.4 index**, based on average sea-surface temperature (SST) anomalies ΔT . [Data courtesy of <https://www.esrl.noaa.gov/psd/enso/dashboard.html>.]
- (b) **Southern Oscillation Index (SOI)**, based on sea-level pressure (SLP) difference: $\Delta P = P_{\text{Tahiti}} - P_{\text{Darwin}}$ [Data courtesy of <https://www.esrl.noaa.gov/psd/enso/dashboard.html>.]
- (c) **Pacific Decadal Oscillation (PDO) index**, based on the leading principal component for monthly Pacific SST variability north of 20°N latitude after global mean SST is removed. [Data courtesy of <https://www.esrl.noaa.gov/psd/enso/dashboard.html>.]
- (d) **North Atlantic Oscillation (NAO) index**, based on the difference of normalized SLP (defined on p 824):
 $\Delta P^* = P^*_{\text{Azores}} - P^*_{\text{Iceland}}$ for winter (Dec - Mar) [Data courtesy of Jim Hurrell, NCAR/CGD/CAS.]
- (e) **Arctic Oscillation (AO) index**, based on the leading principal component of winter SLP in the N. Hemisphere for winter (Jan-Mar) [Data courtesy of Todd Mitchell of the Univ. of Washington Joint Inst. for Study of the Atmos. & Ocean (US JISAO).]

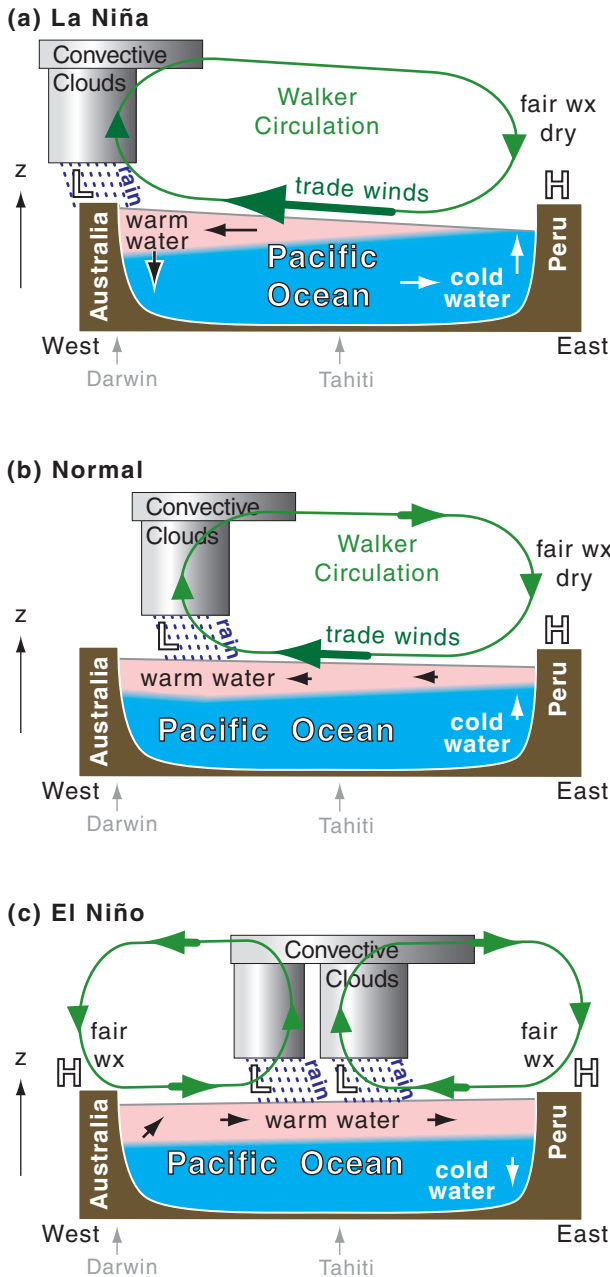


Figure 21.28

Processes that drive ENSO. (a) *La Niña* conditions, where cold upwelling nutrient-rich water off the coast of Peru enables increases in fish populations. Also, cool equatorial water upwells near the central Pacific. Strong trade winds. (b) Normal conditions, with modest trade winds. (c) *El Niño* conditions, associated with a warm-water anomaly in the eastern Pacific, and a decline in fish stocks there. H and L indicate centers of high and low atmospheric pressure, respectively.

The **Southern Oscillation** refers to a change in sign of the east-west atmospheric pressure gradient across the tropical Pacific and Indian Oceans. One indicator of this pressure gradient is the sea-level pressure difference between Tahiti (an island in the central equatorial Pacific, Fig. 21.26) and Darwin, Australia (western Pacific). This indicator ($\Delta P = P_{Tahiti} - P_{Darwin}$) is called the **Southern Oscillation Index (SOI)**.

The SOI, plotted in Fig. 21.27b, varies oppositely to (i.e., is negatively correlated with) the El Niño index (Fig. 21.27a). The reason for this correlation is that El Niño (EN) and the Southern Oscillation (SO) are, respectively, the ocean and atmospheric signals of the same coupled phenomenon, abbreviated as ENSO.

During normal and *La Niña* conditions, the east-to-west decrease in air pressure drives the easterly trade winds, which drag much of the warm ocean-surface waters to the west side of the Pacific basin (Fig. 21.28a). The trade winds are part of the **Walker Circulation**, which includes cloudy rainy updrafts over the warm SST anomaly in the western tropical Pacific, a return flow aloft, and fair-weather (“fair wx”) dry downdrafts. Heavy rain can fall over Australia. Other changes are felt around the world, including cool winters over northern N. America, with drier warmer winters over the southern USA.

During *El Niño*, this pressure gradient breaks down, causing the trade winds to fail, and allowing anomalously warm western Pacific waters to return to the eastern Pacific (Fig. 21.28c). Thunderstorms and rain tend to be strongest over the region of warmest SST. As the SST anomaly shifts eastward, droughts (allowing wild fires) occur in Australia, and heavy rains (causing floods and landslides) occur in Peru. Other changes are felt around the world, including warm winters over northern N. America and cool, wet winters over southern N. America.

21.8.2. Pacific Decadal Oscillation (PDO)

The PDO is a 20- to 30-year variation in the extratropical SST (Fig. 21.27c) near the American coast in the NE Pacific. It has a warm or positive phase (i.e., warm in the key place sketched in Fig. 21.26) and a cool or negative phase. The PDO signal is found using a statistical method called **principal component analysis (PCA)**, also called **empirical orthogonal function analysis, EOF**; see the INFO box on the next three pages.)

The PDO affects weather in northwestern North America as far east as the Great Lakes, and affects the salmon production between Alaska and the Pacific Northwest USA. There is some debate among scientists whether the PDO is a statistical artifact associated with the ENSO signal.

INFO • PCA and EOF

Principal Component Analysis (PCA) and **Empirical Orthogonal Function (EOF)** analysis are two names for the same statistical analysis procedure. They are a form of data reduction designed to tease out dominant patterns that naturally occur in the data. Contrast that with Fourier analysis, which projects the data onto sine waves regardless of whether the data naturally exhibits wavy patterns or not.

You can use a spreadsheet for most of the calculations, as is illustrated here with a contrived example.

1) The Meteorological Data to be Analyzed

Suppose you have air temperature T measurements from different locations over the North Pacific Ocean. Although PCA works for any number of locations, we will use just 4 locations for simplicity:

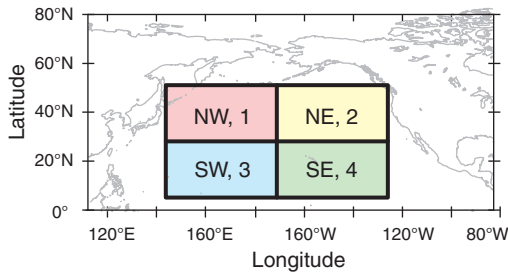


Fig. 21.a. Locations for weather data.

These 4 locations might have place names such as Northwest quadrant, Northeast quadrant, etc., but we will index them by number: $j = 1$ to 4. You can number your locations in any order.

For each location, suppose you have annual average temperature for $N = 10$ years, so your raw input data on a spreadsheet might look this:

Location Index:	j = 1	2	3	4
Location:	NW	NE	SW	SE
Year	Air Temperature (°C)			
i = 1	0	3	8	5
2	4	7	6	8
3	0	6	6	7
4	4	9	5	8
5	0	8	5	6
6	0	9	6	6
7	4	2	10	4
8	0	4	9	4
9	4	6	8	5
10	0	7	5	5
Average:	1.6	6.1	6.8	5.8

(continues)

INFO • PCA and EOF (continuation)

These meteorological data are plotted below:

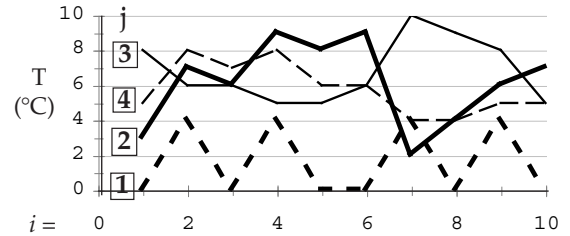


Fig. 21.b. Graphs of raw data at each of 4 locations, where numbers in boxes indicate the j index for each line, and $i = 1$ to 10 years.

Looking at this data by eye, we see that location 2 has a strong signal. Location 4 varies somewhat similarly to 2 (i.e., has positive correlation); location 3 varies somewhat oppositely (negative correlation). Location 1 looks uncorrelated with the others.

2) Preliminary Statistical Computations

Next, use your spreadsheet to find the average temperature at each location (shown at the bottom of the previous table). Then subtract the average from the individual temperatures at the same locations, to make a table of temperature **anomalies** T' :

$$T'_i = T_i - T_{avg} \tag{21.48}$$

Location	j= 1	2	3	4
Year	Air Temperature Anomalies T' (°C)			
i= 1	-1.6	-3.1	1.2	-0.8
2	2.4	0.9	-0.8	2.2
3	-1.6	-0.1	-0.8	1.2
4	2.4	2.9	-1.8	2.2
5	-1.6	1.9	-1.8	0.2
6	-1.6	2.9	-0.8	0.2
7	2.4	-4.1	3.2	-1.8
8	-1.6	-2.1	2.2	-1.8
9	2.4	-0.1	1.2	-0.8
10	-1.6	0.9	-1.8	-0.8

[Check: The average of each T' column should = 0.]

The covariance between variables A and B is:

$$\text{covar}(A,B) = \frac{1}{N} \sum_{i=1}^N A_i \cdot B_i \tag{21.49}$$

where $\text{covar}(A,A)$ is the variance. Use a spreadsheet to compute a table of covariances, where T1 are the temperatures at location $j=1$, T2 are from location 2, etc.:

covar(T1,T1)	covar(T1,T2)	covar(T1,T3)	covar(T1,T4)
covar(T1,T2)	covar(T2,T2)	covar(T2,T3)	covar(T2,T4)
covar(T1,T3)	covar(T2,T3)	covar(T3,T3)	covar(T3,T4)
covar(T1,T4)	covar(T2,T4)	covar(T3,T4)	covar(T4,T4)

(continues)

INFO • PCA and EOF (continuation)

The numbers in that table are symmetric around the main diagonal, so you need to compute the covariances for only the black cells, and then copy the appropriate covariances into the grey cells.

This table is called a **covariance matrix**. When I did it in a spreadsheet, I got the values below:

<u>3.84</u>	-0.16	0.72	0.72
-0.16	<u>5.29</u>	-3.48	2.22
0.72	-3.48	<u>2.96</u>	-1.74
0.72	2.22	-1.74	<u>1.96</u>

The underlined values along the main diagonal are the variances. The sum of these diagonal elements (known as the **trace of the matrix**) is a measure of the total variance of our original data (= 14.05 °C²).

3) More Statistical Computations

Next, find the **eigenvalues** and **eigenvectors** of the covariance matrix. You cannot do that in most spreadsheets, but other programs can do it for you.

I used a website: http://www.arndt-bruenner.de/mathe/scripts/engl_eigenwert2.htm where I copied my covariance matrix into the web page, and specified the eigenvectors to have absolute value of 1. It gave back the following info, which I pasted into my spreadsheet. Under each eigenvalue is the corresponding eigenvector.

k=	1	2	3	4
Eigenvalues (largest first)				
	8.946	4.118	0.740	0.247
Eigenvectors (columns under values)				
j=1	-0.049	0.959	-0.144	-0.238
2	0.749	0.031	-0.579	0.323
3	-0.548	0.126	-0.267	0.782
4	0.369	0.251	0.757	0.477

The sum of all eigenvalues = 14.05 °C² = the total variance of the original data. Those eigenvectors with the largest eigenvalues explain the most variance. Eigenvectors are dimensionless.

4) Find the Principal Components

Next, compute the **principal components** (PCs) — one for each eigenvector (*vect*). The number of eigenvectors ($K = 4$ in our case) equals the number of locations ($J = 4$ in our case).

Each PC will be a column of N numbers ($i = 1$ to 10 in our case) in our spreadsheet. Compute each of these N numbers in your spreadsheet using:

$$PC(k, i) = \sum_{j=1}^J [vect(k, j) \cdot T(j, i)] \quad (21.50)$$

For each variable (T data; eigenvectors; PCs) used in eq. (21.50), the first index indicates the column and the second indicates the row. (continues)

INFO • PCA and EOF (continuation)

Namely:

- k indicates which PC it is ($k = 1$ for the first PC, $k = 2$ for the second PC, up through $k = 4$ in our case) and also indicates the eigenvector (*vect*).
- i is the observation index ($i = 1$ to N , where $N = 10$ yrs in our case), and indicates the corresponding element in any PC.
- j is the data variable index (1 for NW quadrant, etc.), and indicates an element within each eigenvector.

For example, focus on the first PC (i.e., $k = 1$; the first column in the table below). The first row ($i = 1$) is computed as:

$$PC(1,1) = -0.049 \cdot 0 + 0.749 \cdot 3 - 0.548 \cdot 8 + 0.369 \cdot 5 = -0.29$$

For the second row ($i = 2$), it is:

$$PC(1,2) = -0.049 \cdot 4 + 0.749 \cdot 7 - 0.548 \cdot 6 + 0.369 \cdot 8 = 4.71$$

Each PC element has the same units as the original data (°C in our case). The resulting PCs are:

k =	1	2	3	4
	PC1	PC2	PC3	PC4
i=1	-0.29	2.36	-0.08	9.61
2	4.71	6.82	-0.17	9.81
3	3.79	2.70	0.23	9.97
4	6.76	6.75	-1.06	9.68
5	5.46	2.38	-1.42	9.35
6	5.66	2.54	-2.26	10.46
7	-2.70	6.16	-1.37	9.42
8	-0.46	2.26	-1.68	10.24
9	1.76	6.29	-2.39	9.63
10	4.34	2.10	-1.60	8.55
evalue:	8.946	4.118	0.740	0.247

Each PC applies to the whole data set, not just to one location. These PCs, plotted below, are like alternative T data:

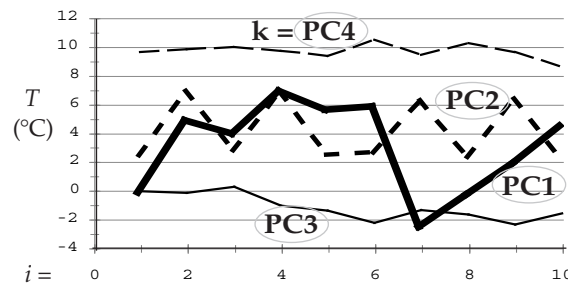


Fig. 21.c. PCs, where $i = 1$ to 10 years.

- PC1 captures the dominant pattern that is in the raw data for locations 2, 3, and 4. This 1st PC explains $8.946/14.05 = 63.7\%$ of the original total variance.
- PC2 captures the oscillation that is in the raw data for location 1. Since location 1 was uncorrelated with the other locations, it couldn't be captured by PC1, and hence needed its own PC. The 2nd PC explains $4.118/14.05 = 29.3\%$ of the variance.
- PC3 captures a nearly linear trend in the data.
- PC4 captures a nearly constant offset.

(continues)

INFO • PCA and EOF (continuation)

5) Synthesis

Now that we've finished computing the PCs, we can see how well each PC explains the original data. Let T_k be an approximation to the original data, re-constructed using only the k^{th} single principal component. Such reconstruction is known as **synthesis**.

$$T_k(j, i) = \text{vect}(k, j) \cdot PC(k, i) \quad (21.51)$$

using the same (column, row) notation as before.

For $k = 1$ (the dominant PC), the reconstructed T_1 data is:

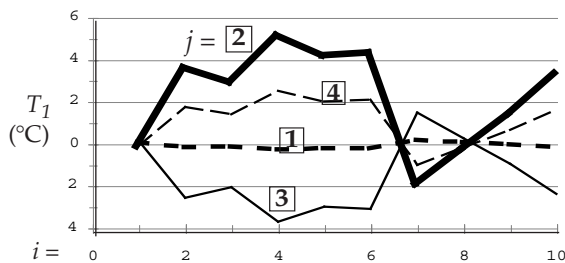


Fig. 21.d. Reconstruction of temperature for each geographic location $j = 1$ to 4 (boxed numbers), but using only the 1st PC. $i = 1$ to 10 years.

It is amazing how well just one PC can capture the essence (including positive and negative correlations) of the signal patterns in the raw data.

The spatial pattern associated with PC1 can be represented on a map by the elements of the first eigenvector [namely, the first eigenvector column in section (3) arbitrarily scaled by 100 here & rounded]:

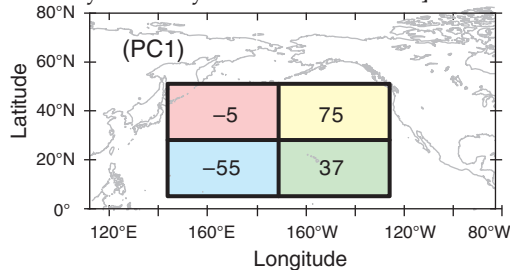


Fig. 21.e. Geographic pattern of influence of PC1.

6) Interpretation:

A dominant pattern in the NE quadrant extends in diminished form to the SE quadrant, with the SW quadrant varying oppositely. But this pattern is not experienced very much in the NW quadrant. Similar maps can be created for the other eigenvectors. When data from more than 4 stations are used, you can contour the eigenvector data when plotted on a map.

Eq. (21.51) can also be used to partially reconstruct the data based on only PC2 (i.e., $k = 2$). As shown in Fig. 21.f, you won't be surprised to find that it almost completely captures the signal in the NW quadrant ($j = 1$), but doesn't explain much in the other regions.

(continues)

INFO • PCA and EOF (continuation)

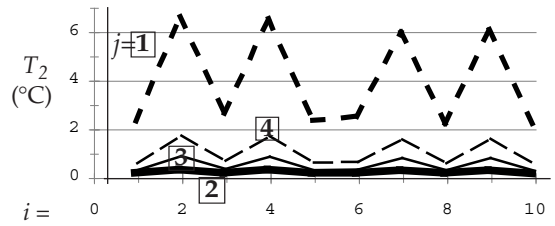


Fig. 21.f. Similar to Fig. 21.d, but using only PC2.

Plotting the elements of the 2nd eigenvector (from section 3; scaled by 100 and rounded) on a map at their geographic locations:

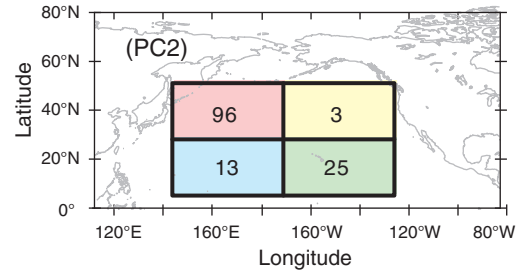


Fig. 21.g. Geographic pattern of influence of PC2.

7) Data Reduction

Suppose that you compute graphs similar to Figs. 21.d & 21.f for the other PCs, and then add all location 1 curves from each PC. Similarly, add all location 2 curves together, etc. The result would perfectly synthesize the original data as was plotted in Fig. 21.a. Although the last 2 PCs don't explain much of the variance (fluctuations of the raw data), they are important to get the mean temperature values.

But what happens if you synthesize the temperature data with only the first 2 PCs (see plot below). These first 2 PCs explain 93% of the total variance. Indeed, the graph below captures most of the variation in the original signals that were in Fig. 21.a, including positive, negative, and near-zero correlations. This allows **data reduction**: We can use only the dominant 2 PCs to explain most of the signals, instead of using all 4 columns of raw data.

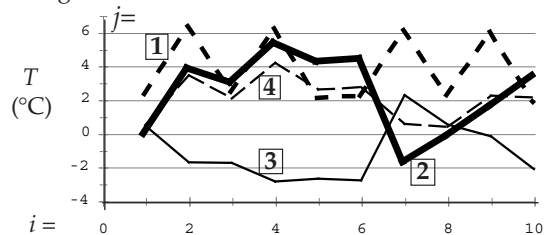


Fig. 21.h. Reconstruction of temperature using only the first 2 PCs.

8) Conclusions

For our small data set, the data reduction might not seem like much, but for larger data sets with hundreds of geographic points, this can be an important way to find dominant patterns in noisy data, and to describe these patterns efficiently. For this reason, PCA/EOF is valued by climate researchers.

21.8.3. North Atlantic Oscillation (NAO)

In the General Circulation chapter (Fig. 11.31) we identified an Iceland low and Azores (or Bermuda) high on the map of average sea-level pressure (SLP). The NAO is a variation in the strength of the pressure difference between these two pressure centers (Fig. 21.26).

Greater differences (called the positive phase of the NAO) correspond to stronger north-south pressure gradients that drive stronger west winds in the North Atlantic — causing mid-latitude cyclones and associated precipitation to be steered toward N. Europe. Weaker differences (negative phase) cause weaker westerlies that tend to drive the extratropical cyclones toward southern Europe.

An NAO index is defined as $\Delta P^* = P^*_{Azores} - P^*_{Iceland}$, where $P^* = (P - P_{clim})/\sigma_P$ is a normalized pressure that measures how many standard-deviations (σ_P) the pressure is from the mean (P_{clim}). The winter average (Dec - Mar) is often most relevant to winter storms in Europe, as plotted in Fig. 21.27d.

21.8.4. Arctic Oscillation (AO)

The AO is also known as the **Northern Annular Mode (NAM)**. It is based on the leading PCA mode for sea-level pressure (SLP) in the N. Hemisphere, and varies over periods of weeks to decades. Fig. 21.27e shows the winter (Jan-Mar) averages.

It compares the average SLP anomaly over the whole Arctic with a pressure anomaly averaged around the 37 to 45°N latitude band. Thus, the AO pattern is zonal, like a bulls-eye centered on the N. Pole (Fig. 21.26). You can think of the NAO as a regional portion of the AO.

Although the AO is measure by SLP, it acts over the whole tropospheric depth, and is associated with the **polar vortex** (a belt of mid-troposphere through lower-stratosphere westerly winds circling the pole over the polar front). The positive, high-index, warm phase corresponds to greater SLP difference between mid-latitudes and the North Pole. This is correlated with faster westerly winds, warmer winter conditions in N. Europe, warmer drier winters in S. Europe, and warmer winters in N. America. The negative, low-index, cool phase has weaker SLP gradient and winds, and opposite precipitation and temperature patterns.

21.8.5. Madden-Julian Oscillation (MJO)

The MJO is 45-day variation (± 15 days) between enhanced and reduced convective (CB) precipitation in the tropics. It is the result of a region of enhanced convection (sketched as the orange shaded oval in Fig. 21.26) that propagates toward the east at roughly 5 to 10 m s⁻¹.

The region of enhanced tropical convection consists of thunderstorms, rain, high anvil cloud tops (cold, as seen by satellites), low SLP anomaly, convergent U (zonal) winds in the boundary layer, and divergent U winds aloft. MJO can enhance tropical cyclone and monsoonal-rain activity. Outside of this region is reduced convection, clearer skies, subsiding air, less or no precipitation, divergent U winds in the boundary layer, convergent U winds aloft, and reduced tropical-cyclone activity.

The convective regions are strongest where they form over the Indian Ocean and as they move eastward over the western and central Pacific Ocean. By the time they reach the eastern Pacific and the Atlantic Oceans, they are usually diminished, although they can still have observable effects.

For example, when the thunderstorm region approaches Hawaii, the moist storm outflow can merge with a southern branch of the jet stream to feed abundant moisture toward the Pacific Northwest USA and SW Canada. This **atmospheric river** of moist air is known as the **Pineapple Express**, and can cause heavy rains, flooding, and landslides due to orographic uplift of the moist air over the coastal mountains (see the Extratropical Cyclone chapter).

A useful analysis method to detect the MJO and other propagating phenomena is to plot key variables on a **Hovmöller diagram** (see INFO box). Eastward-propagating weather features would tilt down to the right in such a diagram. Westward-moving ones would tilt down to the left. The slope of the tilt indicates the zonal propagation speed.

21.8.6. Other Oscillations

Other climate oscillations have been discovered:

- **Antarctic Oscillation (AAO)**, also known as the **Southern Annular Mode (SAM)** in S. Hem. SLP (sketched in Fig. 21.26). 2 - 7 yr variation.
- **Arctic Dipole Anomaly (ADA)**, 2 - 7 yr variation with high SLP over northern Canada and low SLP over Eurasia.
- **Atlantic Multi-decadal Oscillation (AMO)**, 30 - 40 yr variations in SST over the N. Atlantic.
- **Indian Ocean Dipole (IOD)**, 7.5 yr oscillation between warm east and warm west SST anomaly in the Indian Ocean.
- **Interdecadal Pacific Oscillation (IDPO or IPO)** for SST in the N. and S. Hemisphere extratropics. 15-30 yr periods.
- **Pacific North American Pattern (PNA)** in SLP and in 50 kPa geopotential heights.
- **Quasi-biennial Oscillation (QBO)** in stratospheric equatorial zonal winds.
- **Quasi-decadal Oscillation (QDO)** in tropical SST, with 8-12 yr periods.

Other climate variations may also exist.

21.9. REVIEW

Climate is defined as the weather averaged over long periods of time; e.g., 30 yr. Earth’s climate is controlled by both external and internal processes. External processes include the balance between incoming solar radiation and outgoing infrared (IR) radiation. Internal processes include changes to the composition or structure of the atmosphere that alter how energy is distributed within the Earth-ocean-atmosphere-cryosphere-biosphere system.

Externally, changes in Earth’s orbit around the sun as predicted by Milankovitch can alter the amount of sunlight reaching Earth, and changes in the tilt of Earth’s axis can alter the severity of the seasons. Solar output can also vary. Changes in Earth’s average albedo (via snow cover, cloud cover, or coverage of vegetation) can modulate the amount of radiation lost from the Earth system, thereby changing the way that the Earth responds to such external forcings.

Internally, chemicals that normally exist in the atmosphere (water vapor, carbon dioxide, etc.) absorb IR radiation, causing the air to become warmer and re-radiate a large amount of IR radiation back toward the Earth’s surface. This greenhouse effect does not have perfect efficiency, because some wavelength bands of IR radiation can escape directly to space through the so-called “atmospheric window.” Anthropogenic and natural changes to these greenhouse gases can alter the greenhouse efficiency and shift the climate equilibrium — an effect called “climate change.”

Natural internal processes such as volcanic eruptions can also change the climate via emission of sulfates into the stratosphere. Movement of tectonic plates can shift the locations of continents and oceans relative to the equator, altering global-scale and continental-scale (monsoon) circulations and climate.

Some processes in the atmosphere cause negative feedbacks that tend to stabilize the climate, while other positive-feedback processes tend to amplify climate variations. Many of these feedbacks apply to external, internal, natural, and anthropogenic forcings. Overall, our climate is remarkable steady.

Short-term (few years to few decades) variations in Earth’s climate are also observed. El Niño is one example out of many such “oscillations” in the climate signal.

Researchers have classified the current climate (Köppen). They also utilize tools including global climate models (GCMs), principal component analysis (PCA), Hovmöller diagrams, and conceptual models (e.g., daisyworld) to study climate variability.

INFO • Hovmöller Diagram

A Hovmöller diagram is a plot of a meteorological variable as a function of date and longitude. Usually date is along the ordinate — increasing downward. Longitude is along the abscissa. The meteorological variable is contoured with grey or color fill. The latitude or latitudinal band of these meteorological observations is fixed, and is specified in the figure legend or caption. These diagrams are useful for detecting the zonal movement of weather features over time.

For example, suppose that on 1 January you flew an airplane around the world along the equator (0° latitude), and remotely measured the sea surface temperature (SST). After subtracting the average SST, you would be left with a temperature anomaly T' at each point around the equator. Suppose the first graph below shows what you measured.

Later, on 15 January, make the same flight, and plot your measurements (second graph below). Repeat the flights for many different dates.

Instead of plotting each circumnavigation on a separate graph, we can write all the T' numbers on the same diagram of time vs. longitude. Then analyze the result as you learned in the Map Analysis chapter, by drawing isotherms of T' . The result is a Hovmöller diagram (third diagram below). You can use any meteorological variable, not just T' .

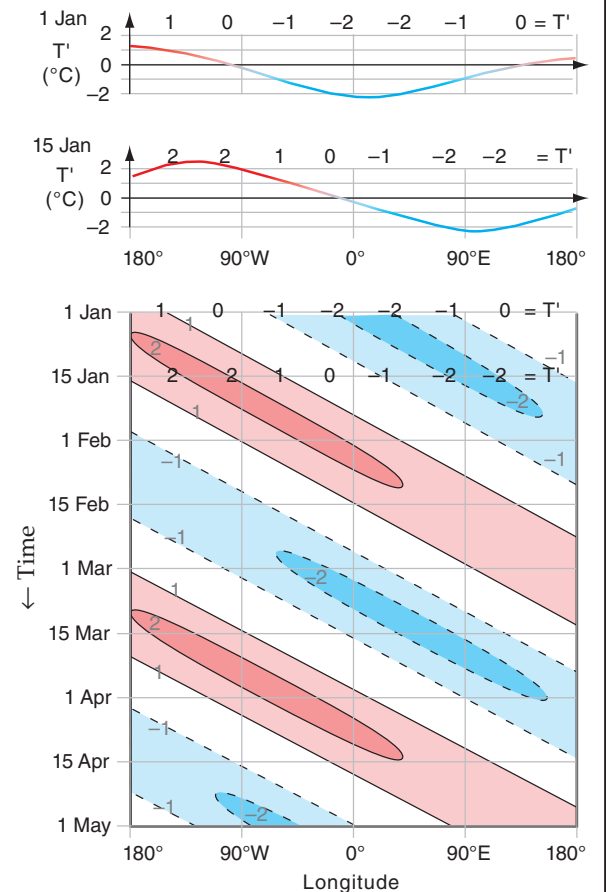


Fig. 21.i Red & blue show positive & negative T' (°C) patterns at the equator that propagate eastward with time.

PERSPECTIVES • Scientific Ethics

It is a worthy human trait to strive to be the best. But for scientists measuring their success by the papers they publish, the temptation to cheat can unfortunately drive people to be unethical.

Such unethical issues have been discussed by C. J. Sindermann (1982: *Winning the Games Scientists Play*. Plenum. 290 pp) and by the Sigma Xi scientific research society (1984: *Honor in Science*. Sigma Xi Pubs., 41 pp):

“• **Massaging** – performing extensive transformations... to make inconclusive data appear to be conclusive;

• **Extrapolating** – developing curves [or proposing theories] based on too few data points, or predicting future trends based on unsupported assumptions about the degree of variability measured;

• **Smoothing** [or **trimming**] – discarding data points too far removed from expected or mean values;

• **Slanting** [or **cooking**] – deliberately emphasizing and selecting certain trends in the data, ignoring or discarding others which do not fit the desired or preconceived pattern;

• **Fudging** [or **forging**] – creating data points to augment incomplete data sets or observations; and

• **Manufacturing** – creating entire data sets *de novo*, without benefit of experimentation or observation.”

Recommendation: Don't cheat. It can mislead colleagues and policy makers, and can ruin your career.

21.10. HOMEWORK EXERCISES

21.10.1. Broaden Knowledge & Comprehension

B1. Search the web for graphs comparing different satellite measurements of the solar irradiance (i.e., the solar constant). Discuss the relative magnitudes of the variation of solar irradiance with time vs. the errors associated with measuring solar irradiance. [Hint: Recall info about accuracy and precision from Appendix A.]

B2. Search the web for maps showing the ice cover on Earth, and how ice cover has changed during the past decades. Discuss these changes in relation to ice-albedo feedback.

B3. Use info from the web to discuss the difference between **Bond albedo** and **geometric albedo**. Which one of these albedos is most appropriate to use for studying the radiation budget of other planets?

B4. Search the web for animations or graphs showing/predicting the changes in eccentricity, obliquity, and precession of the Earth over time. Discuss the simplifications made in these diagrams/animations to communicate this info to the general public.

B5. Search the web for more accurate Earth orbital parameters, to improve and expand the data that were in Tables 21-1 and 21-1b. Save and print this table.

B6. Search the web for accurate graphs of ice ages. Discuss what ice-age details are missing or poorly resolved in the ice-age graph in Fig. 21.8.

B7. Search the web for graphs of solar activity or sunspot number, going as far back in time as you can find. Discuss the regular and irregular components of the sunspot cycle.

B8. Search the web for animations or a sequence of still-frames showing how the continents moved to create Pangea, and how they continued to move into their current configuration. Discuss how monsoonal circulations change and alter the continental climates as the continents move.

B9. Search the web for photos of one recent volcanic eruptions that show: (a) ash fallout close to the volcano, and (b) the plume of aerosols injected into the stratosphere, showing their track around the Earth. Discuss the relative amount of global impact due to the one volcanic eruption.

B10. Search the web for photos of beautiful sunsets that were enhanced by volcanic aerosols in the stratosphere. Read ahead in the Atmospheric Optics chapter to see why you can see red skies and blue moons after some volcanic eruptions.

B11. Search the web for info about other major volcanic eruptions that were not listed in Table 21-3. Discuss the impacts of these eruptions on species.

B12. Search the web for the most recent Assessment Report from the Intergovernmental Panel on Climate Change (IPCC), and identify new information and understanding that updates information in this Chapter.

B13. Search the web for additional climate feedback processes that were not listed in Table 21-4, and discuss their relative importance to the ones already listed.

B14. Search the web for data on actual amounts of global warming during the past two decades, and compare to the predictions presented in older IPCC reports. How accurate are climate predictions?

B15. Search the web for animations of Daisyworld evolution. Enjoy.

B16. Lovelock, the inventor of Daisyworld, wrote a more recent book called "The Revenge of Gaia." If you don't have time to read the book, search the web for a summary of its key points, and argue either for or against his thesis.

B17. Search the web (particularly IPCC Assessment Reports) that summarize the attributes of the various global climate models (GCMs) that were used for the most recent IPCC climate report. Summarize the commonalities and differences between these various GCMs.

B18. Search the web for color maps showing Köppen climate classification for the whole world. Focus on where you live, and discuss how the climate classification does or does not agree with the climate you observed in your area.

B19. Search the web for color diagrams illustrating the processes involved in these climate oscillations:
a. El Niño or ENSO, including the relationship between trade winds, upwelling water, and SST
b. PDO c. NAO d. AO e. MJO

B20. Often climate variations are indicated on **anomaly maps**. An example frequently used for ENSO is the sea-surface-temperature anomaly. (a) Define "anomaly map". (b) Show or give the URL for two other climate anomaly maps on the internet. (c) What is the relationship between sea-surface-temperature anomalies and rainfall shifts or cloud-coverage changes?

B21. Search the web for maps showing the geographic distribution of dominant principal components for any one of the climate oscillations.

B22. Search the web for a Hovmöller diagram for climate oscillations such as MJO in the most recent 6 or 12 months, and analyze it to explain the direction and movement of features.

B23. Based on an internet search, what does the word **teleconnection** mean with respect to phenomena in the global circulation?

B24. Identify the most-recent major El Niño event, and use the internet to identify or catalog 5 of the worldwide consequences (such as storms or fires).

B25. NCEI is a US-government center. What does the acronym mean, and what can this center do for you? List 8 of the main data types you can access.

B26. Search the web graphs showing observed changes in many of the greenhouse gases.

21.10.2. Apply

A1. Find the radiation input to the Earth system for an albedo of:

- a. 0.1 b. 0.15 c. 0.2 d. 0.25 e. 0.35 f. 0.4
g. 0.45 h. 0.5 i. 0.55 j. 0.6 k. 0.65 m. 0.7

A2. Use the albedoes from exercise A1 to calculate the effective radiation temperature of Earth.

A3. For a global albedo of 0.3, find the radiation input to the Earth system for the following total solar irradiances (W m^{-2}):

- a. 1350 b. 1352 c. 1354 d. 1356 e. 1358
f. 1360 g. 1362 h. 1364 i. 1365 j. 1367
k. 1368 m. 1370 n. 1372 o. 1374

A4. Use the solar irradiance values from exercise A3 to calculate the effective radiation temperatures of Earth. Assume the global albedo is 0.3.

A5. Find the net radiation out from the Earth system, for an Earth effective radiation emission temperature ($^{\circ}\text{C}$) of

- a. -19 b. -17 c. -15 d. -13 e. -11
f. -9 g. -7 h. -5 i. -3 j. -1
k. 1 m. 3 n. 5 o. 10 p. 15

A6. Given the planets and dwarf planets listed below, find their effective radiation temperatures.

Planet	Albedo	Planet	Albedo
a. Mercury	0.119	b. Venus	0.90
c. Mars	0.25	d. Jupiter	0.343
e. Saturn	0.342	f. Uranus	0.30
g. Neptune	0.29	h. Pluto	0.40
i. Eris	0.96		

A7. Given an idealized atmosphere having one layer that is totally opaque to infrared radiation, what is the temperature of the planetary surface for:

- (i) exercise A2 (ii) exercise A4 (iii) exercise A6

A8. Given an Earth with an idealized atmosphere having one layer, but with an infrared window, what is the temperature at Earth's surface. Use 255 K as the effective emission temperature, and assume the emissivity is:

- a. 0.70 b. 0.73 c. 0.76 d. 0.80 e. 0.83
 f. 0.86 g. 0.88 h. 0.91 i. 0.93 j. 0.95
 k. 0.97 m. 0.99

A9. Use Fig. 21.6 to answer these questions:

- a. What fraction of energy absorbed at the Earth's surface comes from solar radiation?
 b. What fraction of energy leaving the Earth's surface consists of (latent + sensible) heat?
 c. What is the net flux of IR radiation between the Earth's surface and the atmosphere, and how does this compare to the flux of (latent + sensible) heat?
 d. What is the total amount of upwelling energy (solar, IR, sensible, latent) that reaches the bottom of the idealized atmosphere in that figure?
 e. Why is the 79 W m^{-2} of "solar reflected from atmos." not included in the energy budget of the atmosphere as one of the outgoing fluxes (Hint: See the Sample Application after that figure)?
 f. Why is the (sensible + latent) heat flux upward from the top of the atmosphere not shown?

A10(S). On a very large graph, carefully plot two ellipses. One has eccentricity of 0.0 (i.e., is a circle), and the other has an eccentricity of:

- a. 0.05 b. 0.1 c. 0.15 d. 0.2 e. 0.25 f. 0.3
 g. 0.35 h. 0.4 i. 0.6 j. 0.7 k. 0.8 m. 0.9

A11(S). Using the data from Table 21-1, find the Earth-orbit eccentricity for the following time:

- a. 400 kyr ago b. 1.1 Myr ago c. 1.2 Myr ago
 d. 1.4 Myr ago e. 1.6 Myr ago f. 2 Myr ago
 g. 625 kyr in the future h. 1.1 Myr in future
 i. 1.3 Myr in future j. 2 Myr in future

A12(S). Same as for A11, but find the obliquity ($^\circ$).

A13(S). Same as for A11, but find the climatic precession at the summer solstice (i.e., the $e \sin(\varpi)$ term).

A14(S). Same as for A11 (and A13), but find the ratio of semi-major axis to sun-Earth distance: a/R .

A15(S). Same as A11 (and using your results from A12 - A14), but find the average daily insolation at 65°N during the summer solstice.

A16. Find the sun-Earth distance R (Gm) given an eccentricity of 0.05 and a climatic precession value of: a. -0.05 b. -0.04 c. -0.03 d. -0.02 e. -0.01
 f. 0.01 g. 0.02 h. 0.03 i. 0.04 j. 0.05

A17. Use the definition of optical depth from the Beer's Law section of the Radiation chapter to estimate the optical depth for background "clean" air, which transmits about 94% of incident solar radiation. Also, use data from Fig. 21.17 on recent volcanic eruptions, and compare the "clean" optical depth to the optical depth for:

- a. Mt. Agung (Indonesia)
 b. Mt. Fuego (Guatemala)
 c. El Chichon (Mexico)
 d. Mt. Pinatubo (Philippines)

A18. Find the feedback factor, gain, and system response, given a no-feedback response of $r_o = 0.2$, and a feedback value (F) of:

- a. -8 b. -6 c. -4 d. -2 e. 1 f. 2 g. 3
 h. 4 i. 5 j. 6 k. 7 m. 8 n. 9 o. 10

A19. Based on the answer to A18, is the feedback negative, stable positive, or run-away positive?

A20. For a no-feedback reference state for Earth, find the no-feedback climate response r_o for a blackbody Earth equilibrium radiative temperature of T_e^* (K):

- a. 200 b. 210 c. 220 d. 230 e. 240 f. 250
 g. 260 h. 270 i. 280 j. 290 k. 300 m. 310

A21. Given a reference Earth blackbody radiative temperature of $T_e^* = 255 \text{ K}$ and a reference albedo of $A^* = 0.3$. Find the feedback factor, gain, and total system response if ice-albedo feedback behaves such that the change of Earth albedo (associated with ice coverage changes) with surface temperature ($\Delta A/\Delta T = -c$), where c (K^{-1}) has a value of:

- a. 0.002 b. 0.005 c. 0.008 d. 0.012 e. 0.015
 f. 0.02 g. 0.03 h. 0.05 i. 0.10 j. 0.2

A22. Suppose that doubling of CO_2 in the global atmosphere had the same effect as increasing the incoming solar radiation by $\Delta R_o = 4 \text{ W m}^{-2}$ (due to the increased absorption of solar radiation, as explained in the INFO box on Climate Sensitivity). Given Table 21-4, how much would Earth's equilibrium temperature change (i.e., find ΔT_e in $^\circ\text{C}$) for a reference response with no feedbacks, and for the following feedback process:

- a. water-vapor only b. lapse-rate only
 c. cloud only d. surface-albedo only
 e. all of a - d combined

A23(S). Program the Daisyworld equations into your spreadsheet. Calculate the surface temperature (K), coverage of white daisies, and coverage of black daisies, for luminosity of:

- a. 0.9 b. 1.0 c. 1.1 d. 1.2 e. 1.3
 f. 1.4 g. 1.5 h. 1.6 i. 1.7 j. 1.8

- A24. Describe the climate at
- Oregon coast
 - Olympic Mtns (NW corner of Washington)
 - central Vancouver Island (British Columbia)
 - at the USA-Canada border labels in Fig. 21.25
 - north-central California
 - north-central Idaho
 - western Nevada
 - extreme SE California
 - central part of Alberta (portion shown in map)
 - south central Idaho

21.10.3. Evaluate & Analyze

E1. Derive an equation for the temperature at Earth's surface vs. the effective radiation temperature, assuming two concentric atmospheric layers that are both opaque to infrared radiation. Hint, consider the methods in the Greenhouse-effect subsection.

E2. Modify the derivations from the Greenhouse-effect subsection to calculate the Earth-surface temperature, given a volcanic-ash-filled single-layer atmosphere that absorbs all IR radiation and absorbs 25% of the solar radiation that tries to move through it. Assume surface albedo is unchanged.

E3. Looking at estimates of past temperatures, the global climate 102 Myr ago was about 2 - 5 °C warmer than present, while 2 Myr ago the global climate was 1.5 - 3.0°C cooler. Is our current "global warming" approaching the normal climate, or is it deviating further away. Discuss.

E4. Explain how the "atmospheric window" in Fig. 21.5 relates to Figs. 8.3 and 8.4 in the Satellites & Radar chapter.

E5. Consider the heat/energy fluxes shown in Fig. 21.6. Assume an atmosphere with a single opaque layer. What if the sun suddenly gets hotter, causing incoming solar radiation to increase by 50%.

Which of the fluxes would change the quickest and which the slowest? How would the new climate equilibrium compare to Earth's present climate?

E6. In music there is a concept of "**beat frequency**". Namely, when two sounds are produced that have nearly the same tone (frequency), you can hear a third tone that depends on the difference between the two frequencies. Look-up the definition of "beat frequency", and use that info to explain why the Climatic Precession curve in Fig. 21.8 looks the way it does.

E7. a. Given the max and min values of climatic precession plotted in Fig. 21.8, what are the max and min of values of (a/R) ; namely, the ratio of semi-major axis to sun-Earth distance?

b. Simplify the equation (21.18) for the solar declination angle for the special case of the summer solstice.

c. Given the max and min of obliquities plotted in Fig. 21.8, what are the max and min of solar declination angles (°) for the summer solstice?

d. Combine the info in Figs. 21.11 - 21.13 to estimate the max and min values of solar irradiance ($W m^{-2}$) during the past 1000 years.

e. Given your answers to (a) - (d) above, which has the largest effect on the value of daily-average insolation at 65°N during the summer equinox: climatic precession, obliquity, eccentricity, or solar irradiance?

E8. In Fig. 21.8, the Daily Average Insolation graph is based on a combination of the previous three graphs in that figure. Looking at the nature of the signals in all four top graphs in Fig. 21.8, which of the top 3 graphs best explains the Insolation, and which of the top 3 least explain the Insolation? Why?

E9(§). Table 21-1 shows only the first $N = 4$ or 5 terms for Earth's orbital factors. Use all the terms in Table 21-1b, on the next page to calculate and accurately reproduce the first 3 graphs in Fig. 21.8.

E10. Use the orbital data for Earth to answer the following. How many years in the future is the first time when the perihelion will coincide with the summer solstice? This is important because it means that summers will be hotter and winters colder in the N. Hemisphere, because the N. Hemisphere will be tilted toward the sun at the same date that the Earth is closest to the sun.

E11 Show that the right-hand approximation in eq. (21.18) for the solar declination is the same as eq. (2.5). [Hints: Consider that in summer, Earth is 90° further along its orbit than it was in Spring. Use trig identities that relate sines to cosines. Consider the definitions of various orbital angles, as summarized in the INFO box on Sun-Earth Distance.]

E12. Explain why Pangea's climate would be different than our present climate. [Hint: Consider global circulations and monsoonal circulations, as discussed in the General Circulation chapter.]

E13. a. Use the definitions of optical depth and visual range from the Beer's Law section of the Solar &

Table 21-1b. Factors in orbital series approximations.

index	A	P (years)	ϕ (degrees)
Eccentricity:			
i= 1	0.010739	405,091.	170.739
2	0.008147	94,932.	109.891
3	0.006222	123,945.	-60.044
4	0.005287	98,857.	-86.140
5	0.004492	130,781.	100.224
6	0.002967	2,373,298.	-168.784
7	0.002818	977,600.	57.718
8	0.002050	105,150.	49.546
9	0.001971	486,248.	148.744
10	0.001797	688,038.	137.155
11	0.002074	100,805.	24.487
12	0.001525	76,909.	102.380
13	0.001491	134,300.	-167.676
14	0.001316	103,158.	69.234
15	0.001309	118,077.	-51.163
16	0.001300	109,936.	-146.081
17	0.001306	127,123.	-139.827
18	0.001261	55,002.	30.098
19	0.001344	96,727.	27.612
20	0.001058	346,318.	178.662
Obliquity:			
j= 1	0.582412°	40,978.	86.645
2	0.242559°	39,616.	120.859
3	0.163685°	53,722.	-35.947
4	0.164787°	40,285.	104.689
5	0.095382°	41,697.	-112.872
6	0.094379°	41,152.	60.778
7	0.087136°	9,572,151.	39.928
8	0.064348°	29,842.	-15.13
9	0.072451°	28,886.	-155.175
10	0.080146°	40,810.	-70.983
11	0.072919°	41,319.	10.533
12	0.033666°	39,465.	-31.614
13	0.033722°	39,784.	77.554
14	0.030677°	40,455.	71.757
15	0.039351°	29,768.	145.835
16	0.030375°	29,926.	160.109
17	0.024733°	29,690.	144.926
18	0.025201°	40,622.	-173.656
19	0.021615°	41,880.	-144.933
20	0.021565°	54,030.	-79.670
21	0.021270°	53,426.	-178.441
22	0.021851°	40,108.	-24.566
23	0.014725°	28,997.	124.744
Climatic Precession:			
k= 1	0.018986	23,682.	44.374
2	0.016354	22,374.	-144.166
3	0.013055	18,953.	154.212
4	0.008849	19,105.	-42.250
5	0.004248	23,123.	90.742
6	0.002742	19,177.	61.600
7	0.002386	19,025.	74.660
8	0.001796	22,570.	-145.502
9	0.001908	19,260.	119.333
10	0.001496	16,465.	141.244
11	0.001325	18,804.	169.748
12	0.001266	23,178.	-110.52
13	0.001165	18,873.	-78.477
14	0.001304	22,425.	-161.509
15	0.001071	22,528.	16.058
16	0.000970	22,323.	47.804
17	0.001002	23,064.	126.199
18	0.000936	19,334.	38.272
19	0.000781	19,417.	-77.364
20	0.000687	18,656.	14.412
21	0.000575	24,199.	134.011
22	0.000577	19,146.	-99.821
23	0.000651	22,639.	130.819
24	0.000416	22,938.	188.622
25	0.000497	22,600.	109.059
26	0.000392	23,233.	46.89

Simplified from Laskar, Robutel, Joutel, Gastineau, Correia & Levrard, 2004: A long-term numerical solution for the insolation quantities of the Earth. "Astronomy & Astrophysics", 428, 261-285.

IR Radiation chapter to find a relationship for visibility (km) as a function of optical depth τ .

b. Use your answer from (a) with the data from Table 21-3 to estimate the atmospheric visibilities associated with the following volcanic eruptions:

- (i) Lake Toba (ii) Mt. Tambora (iii) Krakatau

E14. For every type of climate feedback, explain why runaway climate change is not possible. [Or if it is possible, show how runaway climate changes applies for only a limited change of Earth temperatures before a new stable climate equilibrium is reached. Can you recall any Hollywood movies that showed runaway climate change, with or without reaching a stable equilibrium?]

E15. For the feedback interconnections shown in Fig. 21.18, the feedback outcomes are only: negative (damped), positive (amplified), or runaway (increasing without limit). Can you think of a different type of interconnection or process that could cause the system response to oscillate? Explain.

E16. Ice-albedo processes were used for an idealized illustration of feedback. Try to develop your own feedback concepts that account for the following (and ignores all other feedbacks except the fundamental radiative feedback). Suppose there is a CO₂ feedback process whereby warmer Earth temperatures cause the oceans to release more CO₂ into the air. But more CO₂ in the air acts to partially close the IR window sketched in Fig. 21.5.

a. What info or what relationships do you need to be able to figure out the feedback? [Only list the info needed — do not actually find these relationships.]

b. If you are good at calculus and if assigned by your instructor, then try to create a governing equation similar to that used for ice-albedo feedback, then take the derivatives as was done in the Higher Math Feedback Example box. There is no single correct answer — many different approximations and solutions might be reasonable. Justify your methods.

E17. For feedbacks in the Earth climate system, use error-propagation methods as discussed in Appendix A, to propagate the errors listed in the feedback (F) column of Table 21-4 into the other columns for feedback factor (f), gain (G), & system response (r).

E18. Do outside readings to explain how the following abrupt climate-change processes work (Table 21-4). Also, explain if feedback is positive or negative.

- a. meridional overturning ocean circulation
- b. fast Antarctic & Greenland ice-sheet collapse
- c. volcanoes
- d. biogeochemical
- e. methane release due to hydrate instability and permafrost)

Table 21-8. Names of Köppen climate classes.

Exercise	Code	Name
a	Af	equatorial climate
b	Am	monsoon climate
c	Aw	tropical savanna climate
d	BWh	warm desert climate
e	BWk	cold desert climate
f	BSh	warm semi-arid climate (warm steppe clim.)
g	BSk	cold semi-arid climate (cold steppe climate)
h	Csa	warm mediterranean climate
i	Csb	temperate mediterranean climate
j	Cwa	warm humid subtropical climate
k	Cwb	temperate humid subtropical climate
l	Cwc	cool humid subtropical climate
m	Cfa	warm oceanic/marine; or humid subtropical
n	Cfb	temperate oceanic/marine climate
o	Cfc	cool oceanic/marine climate
p	Dsa	warm continental (mediterranean continental)
q	Dsb	temperate continental (mediter. continental)
r	Dsc	cool continental climate
s	Dsd	cold continental climate
t	Dwa	warm humid continental climate
u	Dwb	temperate humid continental climate
v	Dwc	cool continental clim.; cool subarctic climate
w	Dwd	cold continental clim.; cold subarctic climate
x	Dfa	warm humid continental climate
y	Dfb	temperate humid continental climate
z	Dfc	cool continental clim.; cool subarctic climate
aa	Dfd	cold continental clim.; cold subarctic climate
ab	ET	tundra climate
ac	EF	ice cap climate

- E19.(§) For a daisyworld
- Redo the calculation shown in this chapter.
 - What happens to the temperature over black and white daisies if transport Tr changes to 0 or 1?
 - What happens if you start with initial conditions of 100% coverage by white or black daisies?
 - What happens if you take a time step increment of 2, 4, or 8?
 - What parameter values prevent homeostasis from occurring (i.e., eliminate the nearly constant temperature conditions on a fecund daisyworld)?
 - Is it possible for homeostasis to occur on Earth, given the large fraction of area covered by oceans?

E20(§). In Fig. 21.24 for Daisyworld, homeostasis is possible for luminosities spanning only a certain range. What changes to the daisy growth parameters or equations would permit homeostasis for luminosities spanning a greater range? Confirm your results by solving the resulting Daisyworld equations with your new parameters.

Table 21-9. Time series for PCA exercise.

Location Index:	j = 1	2	3	4
Location:	NW	NE	SW	SE
Year	Air Temperature (°C)			
i = 1	9	1	1	8
2	7	2	1	8
3	5	3	2	7
4	7	4	5	6
5	9	5	9	5
6	7	6	9	5
7	5	5	5	5
8	7	4	5	6
9	9	3	4	7
10	7	2	1	8

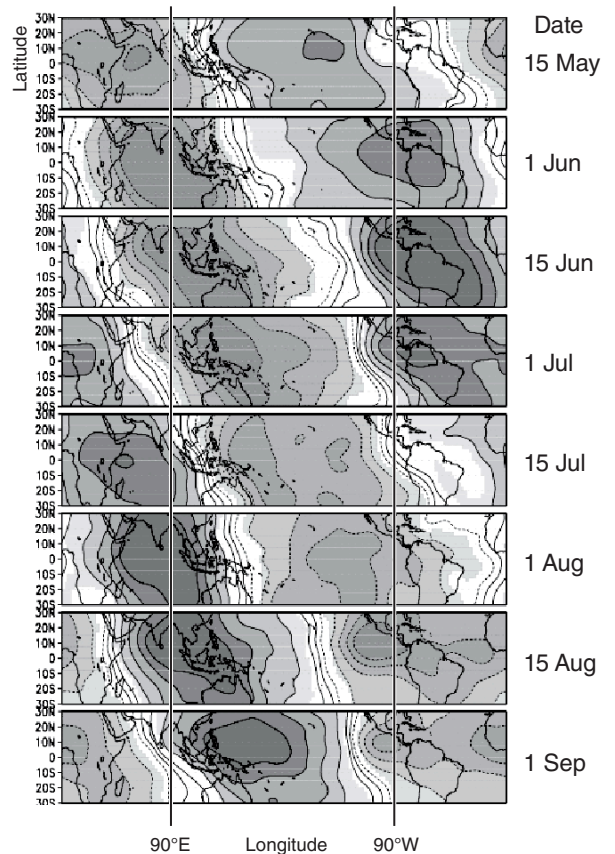


Figure 21.29 Hovmöller Diagram showing 20 kPa winds. (Shading is arbitrary for this exercise.) Modified from data courtesy of the Climate Prediction Center, National Weather Service, National Oceanic and Atmospheric Admin.

E21. Where in the world (but NOT in any region plotted in Fig. 21.25) would you expect to find the climate in Table 21-8 above. (Hint, consider info in the General Circulation chapter, and also use the Köppen climate definitions in Table 21-6.)

E22(§-difficult). Find the covariance matrix, the eigenvectors and eigenvalues (using some other resource such as a web-based eigenvector calculator), leading 2 principal components (PCs), interpret the results, and reconstruct (synthesize) the original data as approximated using the dominant 2 PCs, given time series in Table 21-9. Assume that the locations for these time series correspond to the geographic locations shown in Fig. 21.a of the PCA INFO box.

E23. Given the Hovmöller diagram in Fig. 21.29, determine the zonal speed and direction (toward east or west) that features move.

21.10.4. Synthesize

S1. What if emitted IR radiation were constant — not a function of temperature. How would Earth's climate be different, if at all?

S2. Create an energy balance to determine T_s and T_e for an atmosphere with:

- 2 opaque atmospheric layers (no window)
- 3 opaque atmospheric layers (no window)
- extrapolate your theory so it works with more layers

S3. Suppose the same side of the Earth always faced the sun, and the atmosphere was stationary over the Earth. Assume no heat transport between Earth's cold and warm sides. Write the equations (along with your justification) for energy balances for each side of the Earth, for the following scenarios:

- a single-layer opaque atmosphere.
- a single-layer atmosphere, but having an IR window.

S4. Suppose radioactive decay deep inside the Earth caused as much heat transport into the bottom of the atmosphere as is incoming solar radiation into the top of Earth's atmosphere. Work out the energy budgets, and calculate steady-state Earth-surface temperatures. Discuss feedbacks. (Hint, assume a single-layer opaque atmosphere.)

S5. Estimate the variation in insolation if Earth's orbit were to have eccentricity of 0.8.

S6. Given idealized ozone holes centered over each pole, where each hole extends 25° of latitude from the pole. In each hole, assume that the atmosphere is totally transparent to IR radiation. Assume that Earth's climate can be divided in to latitude bands of uniform surface temperature: hot near the equator, temperate at mid latitudes, and cold directly under the ozone holes. (a) Devise energy-balance equa-

tions for each latitude band, (b) find the average surface temperature within each band, and (c) find the overall Earth-surface average temperature. Justify any assumptions you make.

S7. Suppose a long-lasting solar storm ionizes the air and totally closes the infrared window on Earth's sunny side. However, Earth's shady side is not affected, allowing an atmospheric window to exist in the infrared. (a) What is the steady-state Earth-surface temperature (averaged over the whole globe)? (b) Show your budget equations justify your assumptions to support your answer.

S8. For Daisyworld, start with global coverages of 50% dark and 50% light daisies. Assume that no bare ground is allowed at any time, although relative coverage of light and dark daisies can change. (a) Devise equations to describe this scenario, and (b) compare your results with the Daisyworld equations and results earlier in this chapter. (c) Does the new Daisyworld allow homeostasis? (d) Is the new Daisyworld more or less sensitive to changes in luminosity?

S9. If runaway climate change caused the Earth to reach a new warmer equilibrium, would the Earth's climate be able to recover to the climate we currently have? What positive and/or negative feedback processes would encourage such recovery?

- S10. Would global warming alter:
- the global circulation?
 - thunderstorm severity?
 - thunderstorm frequency?
 - hurricane (or typhoon) severity?
 - hurricane (or typhoon) frequency?
 - hurricane (or typhoon) tracks?

Explain how.

S11. Discuss the scientific accuracy of recent Hollywood movies where the theme was weather or climate disasters.

S12. Repeat the principal component analysis from the INFO box, but when you calculate the table of principal components (PC), use the temperature anomaly T' in eq. (21.50) instead of T . Then finish all the remaining calculations using these new PCs.

What is the sum of elements in each PC (i.e., the sum of each column in the PC table)? What is the relationship between your plotted PCs and Fig. 21.c? When you synthesize the signal using only PC1, how does your result compare to Fig. 21.d?

Outcome: you are synthesizing T' and not T . Most researchers use PCA to focus on the anomaly.